ORIGINAL ARTICLE

CrossMark

GIS-based landslide susceptibility evaluation using fuzzy-AHP multi-criteria decision-making techniques in the Abha Watershed, Saudi Arabia

Javed Mallick[1] · Ram Karan Singh[1] · Mohammed A. AlAwadh[2] · Saiful Islam[1] · Roohul Abad Khan[1] · Mohamed Noor Qureshi[2]

Abstract

Landslides are natural geological disasters causing massive destructions and loss of lives, as well as severe damage to natural resources, so it is essential to delineate the area that probably will be affected by landslides. Landslide susceptibility mapping (LSM) is making increasing implications for GIS-based spatial analysis in combination with multi-criteria evaluation (MCE) methods. It is considered to be an effective tool to understand natural disasters related to mass movements and carry out an appropriate risk assessment. This study is based on an integrated approach of GIS and statistical modelling including fuzzy analytical hierarchy process (FAHP), weighted linear combination and MCE models. In the modelling process, eleven causative factors include slope aspect, slope, rainfall, geology, geomorphology, distance from lineament, distance from drainage networks, distance from the road, land use/land cover, soil erodibility and vegetation proportion were identified for landslide susceptibility mapping. These factors were identified based on the (1) literature review, (2) the expert knowledge, (3) field observation, (4) geophysical investigation, and (5) multivariate techniques. Initially, analytical hierarchy process linked with the fuzzy set theory is used in pairwise comparisons of LSM criteria for ranking purposes. Thereafter, fuzzy membership functions were carried out to determine the criteria weights used in the development of a landslide susceptibility map. These selected thematic maps were integrated using a weighted linear combination method to create the final landslide susceptibility map. Finally, a validation of the results was carried out using a sensitivity analysis based on receiver operator curves and an overlay method using the landslide inventory map. The study results show that the weighted overlay analysis method using the FAHP and eigenvector method is a reliable technique to map landslide susceptibility areas. The landslide susceptibility areas were classified into five categories, viz. very low susceptibility, low susceptibility, moderate susceptibility, high susceptibility, and very high susceptibility. The very high and high susceptibility zones account for 15.11% area coverage. The results are useful to get an impression of the sustainability of the watershed in terms of landsliding and therefore may help decision makers in future planning and mitigation of landslide impacts.

Keywords Multi-criteria decision analysis · Fuzzy analytical hierarchy process · Fuzzy membership functions · Geoinformation technology · Landslide susceptibility maps

Introduction

Landslides are natural disaster, significantly affected by the failure of materials making up the hill slopes and are augmented by the force of gravity, precipitation and anthropogenic activities causing massive destruction and loss of lives, in addition to severe loss of natural resources (Intarawichian and Dasananda 2010; Feizizadeh et al. 2014). The spatial probability of landslides, also known as susceptibility, is the probability of a landslide occurring in an area on the basis of local terrain conditions (Brabb 1984; Ilanloo 2011). Susceptibility neither considers the temporal probability of failure (i.e. when or how frequently landslides occur), nor the magnitude of the expected landslide (i.e. how large or destructive the failure will be). Several methods and techniques for evaluating landslide susceptibility have been proposed in the literature (Wang et al. 2012).

✉ Javed Mallick
jmallick@kku.edu.sa

1 Department of Civil Engineering, College of Engineering, King Khalid University, Abha, Saudi Arabia

2 Department of Industrial Engineering, College of Engineering, King Khalid University, Abha, Saudi Arabia

GIS-based spatial analysis coupled with multi-criteria evaluation (MCE) methods is making increasing implications in landslide susceptibility mapping (LSM) studies. It is thought to be a valuable tool for understanding these natural hazards and foreseeing potential landslide hazard areas (Feizizadeh et al. 2014). Thereby, it can assist the decision makers for further planning and mitigation of landslide impacts (Roodposhti et al. 2016).

Various techniques and tools adopted for determining landslide susceptibility can be categorized as subjective and objective methods. The subjective methods consist of inventory mapping and decision makers' assessments using standardization and weighting procedures based on thematic maps (Wang et al. 2012). The subjective approaches used multi-criteria evaluation (MCE) techniques, viz. simple additive weighting (Feizizadeh and Blaschke 2013), ordered weighted average (Ayalew et al. 2004), analytical hierarchy process (Yalcin 2008), analytical network process (Neaupane and Piantanakulchai 2006) and also heuristic and knowledge-based techniques (Barredo et al. 2000). The second technique through the objective method mostly relies on statistical analysis (Lee and Min 2001), soft computing (Lee et al. 2004a, b), deterministic analysis (Carrara 1983), neuro-fuzzy (Pradhan 2013), artificial neural network (Dou et al. 2015), index of entropy (Pourghasemi et al. 2012) and decision trees (Hong et al. 2015). The objective method typically depends on the objective assessments and is more rigorous. Therefore in this study, we adopted subjective approach is an expert-driven qualitative method to assess the landslide susceptibility and to produce a susceptibility map portraying its spatial distribution under GIS environment. LSM needs a multi-criteria method with high levels of precision and dependability in the subsequent maps, with a specific end goal to support decision-making and risk assessment. The effectiveness of decision-making relies on the quality of the data and techniques to develop the landslide susceptibility maps (Wang et al. 2012). GIS-based multi-criteria decision analysis (MCDA) is an important technique that allows data derived from various sources to be consolidated (Feizizadeh et al. 2014). GIS-based MCDA transforms the spatial and non-spatial data into information that can be utilized in decision-making (Chen et al. 2010). The Analytic Hierarchy Process (AHP) method is widely considered for multiple-criteria decision-making (MCDM) and has been successfully used in various areas of natural resource management, environmental impact assessment, and regional planning (Saaty 1980; Ouma and Tateishi 2014; Oikonomidis et al. 2015; Rahaman et al. 2015; Mallick 2016). AHP has gained its significance due to its interactive graphical user (IGU) interfaces, automatic calculation of priorities and variabilities, and sensitivity analysis. Even though its popularity, the method is often criticized for its inability to efficiently handle the inherent uncertainty and imprecision related to the geo-visualization of a decision maker's perception of crisp numbers. The empirical effectiveness and theoretical validity of the AHP have also been discussed by many authors (Mcintyre and Parfitt 1998; Cheung et al. 2002; Chowdhury et al. 2009; Ishizaka and Labib 2011, Wang et al. 2012; Ahmad et al. 2013; Shahabi and Hashim 2015). Many researchers have also been discussed the empirical effectiveness and theoretical validity of the AHP (Mcintyre and Parfitt 1998), and this discussion has consequently focused on four primary domains: the axiomatic foundation, the correct meaning of priorities, the 1–9 measurement scale and the rank reversal problem (Millet and Saaty 2000). Despite that, most of the criticisms in these areas have been partially resolved, mainly three-level hierarchic structures (Hsieh et al. 2004).

The objective of the current study is to propose a method to resolve the uncertainty and imprecision within the analytical hierarchy prioritization process by representing the decision-makers choices as fuzzy numbers or fuzzy sets. In the AHP method, the decision-making problem is organized hierarchically at different levels, each level containing a finite number of elements, but in many situations, the preference model of the decision maker is uncertain and fuzzy, and it is somewhat challenging crisp numerical values of the comparison ratios to be provided by subjective perception. The decision makers may be subjective and uncertain about their level of preference because of incomplete knowledge or information, and uncertainty within the decision environment. AHP can be linked with fuzzy logic methods (Willey 1979; Altrock and Krause 1994; Opricovic and Tzeng 2003; Li and Will 2005) in uncertainty analysis and provide a framework that makes use of the fuzzy membership functions (FMFs) to evaluate the criteria and provide more accurate result (Feizizadeh et al. 2014). The criterion maps are standardized using fuzzy sets in context with the MCDM by assigning to each object a membership or non-membership function of each criterion (Gorsevski and Jankowski 2010). The assessment of results for decision-making using the AHP integrated with fuzzy set theory allows greater flexibility.

The region's climate and geo-physiographic conditions can also determine the likelihood of a landslide and mass wasting events, which occur periodically over time. In the last few years, many efforts of slope stability and landslide susceptibility mapping applied in Saudi Arabia (Youssef et al. 2012, 2013, 2014; Youssef and Maerz 2013; Maerz et al. 2014; Mallick et al. 2014). In the current study, GIS-based statistical models including fuzzy analytical hierarchy process (FAHP), weighted linear combination (WLC) and multi-criteria evaluation (MCE) models were adapted to develop a landslide susceptibility map. There is substantial need to improve the prediction of future landslide areas and risk assessment coupled with geoinformation technology to quantify the risk of landslide hazards zone. The results

obtained from this study provide a considerable contribution to the researchers and practitioners involved in the construction projects dealing with the landslide protection, who may work in the fields of civil engineering, environmental analysis, natural risk hazards and safety management, and decision makers can choose favourable locations for development and conservation schemes.

Study area and geospatial setting

Abha semi-arid mountainous watershed is located in the Aseer Province, Saudi Arabia. The watershed covers an area of 370 km^2 and boundary lies between the latitude of 18°10′12.39″N and 18°23′33.05″N and longitude of 42°21′41.58″E and 42°39′36.09″E. The watershed represents a part of Abha's highland, i.e. related to the Arabian shield in the western part of the Saudi Arabia (Fig. 1). In the Arabian shield, the Precambrian rocks are mostly Neoproterozoic, but in total record 3000 million years of Earth history. According to the Saudi Geological Survey, the watershed area is underlain predominately by upper Proterozoic

metamorphosed volcanic and sedimentary rocks of the Bahah, and Jiddha group and by upper Proterozoic plutonic rocks ranging in composition from Gabbro to granite. This ecoregion characterized by natural geological erosion and sedimentation phenomena of high intensity, as well as man-induced accelerated land degradation processes (Mallick et al. 2014; Youssef et al. 2016).

The study area collects variable rainfall caused by the south-western monsoon, which carries wet oceanic winds (Vincent 2008). This region has the highest average rainfall in Saudi Arabia distributed over 2–4 months during the spring and summer growing seasons (March–June) while rainfall that occurs during the rest of the year is negligible (Wheater et al. 1989). During the raining season, some of its neighbouring villages and rural areas witness flash-floods. The climatic condition in the study area is cold and semi-arid (Koppen:BSk). According to the analysis of rainfall station (ABHA, station no. 41112), operated by the Presidency of Meteorology and Environment (PME) which is located in the southwest of the study area. Rainfall typically occurs in intense thunderstorms from March to June. The maximum monthly precipitations for last 30 years were 43.7,
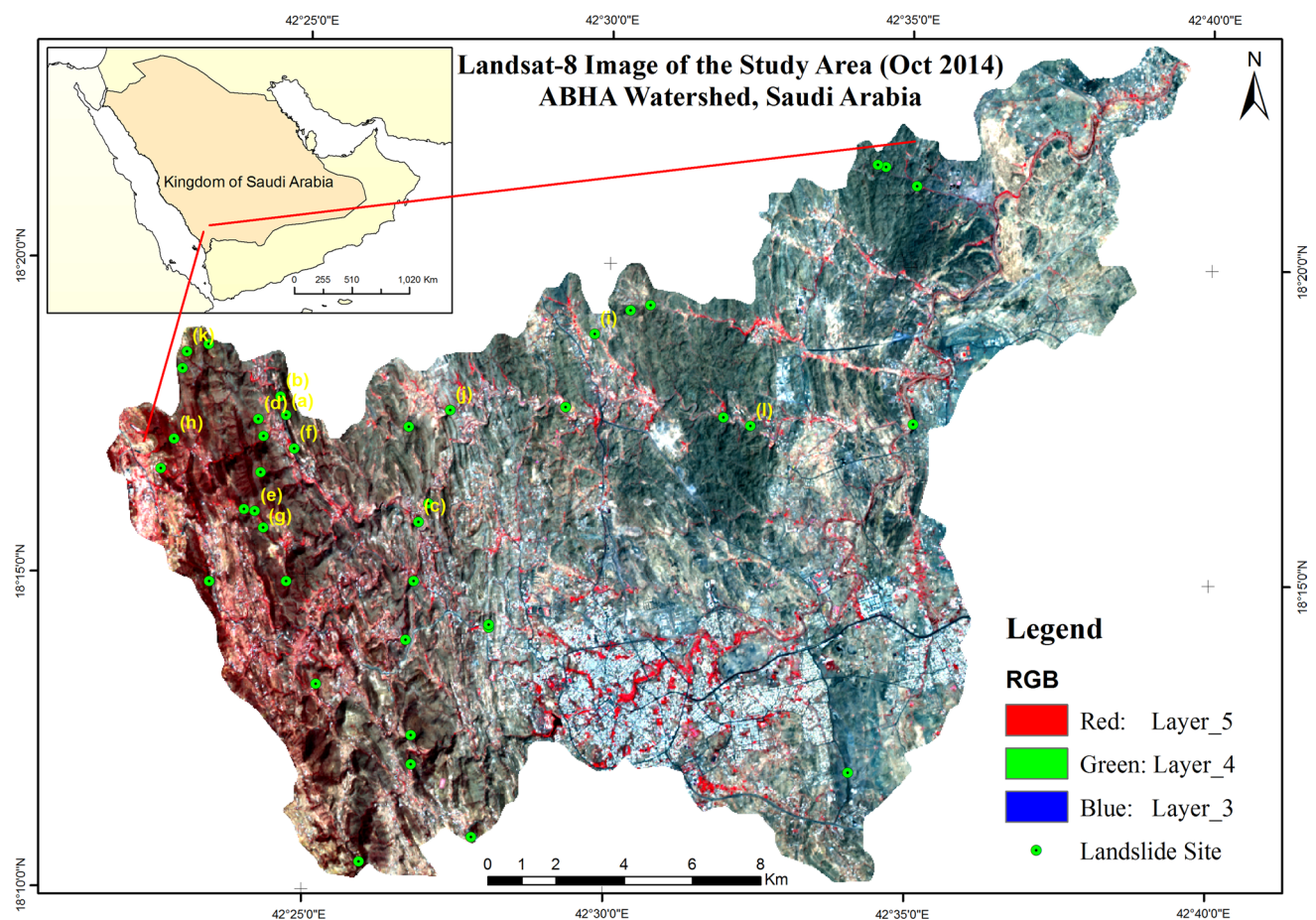

Fig. 1 Study area

244.0, 112.8 and 17.6 mm for March, April, May and June, respectively. The average annual precipitation is reported as about 214 mm/year, with a maximum rainfall of 639.5 mm occurring in 1983. The maximum rainfall occurred in a day was 99 mm in 3 February 1983. The average minimum and maximum temperature is 19.3 and 29.70 °C, respectively. The topography of the area is undulating, and the elevation ranges from 1954 to 2989 m above the sea level. The study area is elongated in shape and dissected by many small wadies (valleys) that drain their waters towards Abha Wadi. The slope angles range from 0° to 52.32°. The watershed has a heterogeneous landscape regarding terrain complexity. The seismic zones in Saudi Arabia situated along the Red Sea and the Gulf of Aden in the west and south and the subduction zone associated with the Zagros suture in the north. In general, the damage and losses associated with earthquakes are negligible in this region (Abdulaziz et al. 2014); the regions along the Red Sea coast are vulnerable to earthquakes. Our study area is situated about 200 km east from the Red Sea hence in the present study area, the internal deformation of the Arabian plate may be insignificant. In the Aseer region, many escarpments roads and highways have been developed all over the regions where the Arabian shield found. These highways and roads connect numerous urban areas located at a high elevation of the mountains with other cities situated along the Red Sea coast. Some of these roads include the road from Abha to the Red Sea coast and local roads in the Jazan region. Along these areas, many rock falls have happened that block the roads, as well as damage infrastructure and cause injuries and fatalities.

The watershed is located in the different geological units, which digitized from the 1:250,000 Abha quadrangle geological map (Greenwood 1985) (Fig. 1). Geologically the area is underlain predominately by upper Proterozoic metamorphosed volcanic and sedimentary rocks of the Bahah, and Jiddha group and by upper Proterozoic plutonic rocks ranging in composition from Gabbro to granite. Eight types of geologic lithology found in the study area.

- Granite Suite–Biotite Monzogranite–Diorite and Gabbro (dg).
- Jiddah Group–Basalt and Andesite–Pillow lava, flow breccia, tuff, dacite tuff, interbedded subordinate, often carbonaceous conglomeratic graywacke and phyllie (jt).
- Sedimentary–Wajid sandstone (Oew).
- Jiddah Group–Bahah group within the Tayyah belt–Volcaniclastic graywacke, carbonaceous, shale and siltstone, subordinate chert, slate, and conglomerate, minnor interbedded basalt, andesite, and dacite (bt).
- Granite Suite–Biotite Monzogranite–Uniform body (grb).
- Jiddah and Bahah group–Biotite-Quartz-Plagioclase Granofels–Subordinate amphibolite, anabiotite schist (jbg)).
- Dioritic and Gabbroic Rocks–Metagabbro (mg).
- Dioritic and Gabbroic Rocks–Gabbro–Massive to layered plutons, sills, dikes, and irregular bodies (gb).

The dominate types of soil class in the study are loamy sand, sandy loam, and loam (Mallick 2016). The study area embraces one of the richest and the most variable floristic regions of Aseer Mountains (Vincent 2008). The variation in climate and topography in the study area (Aseer Province) has led to the formation of diverse plant community (Abulfatih 1981). Foggy cold places are dominated by *Juniperus procera*. Acacia trees are widely distributed to the west of the study area in highlands region. *Ficus salicifolium* communities and *Ziziphus spina-christi var. spina-christi* are common in the lowlands, and many others found on the steep slopes to the west and south of the highlands (Abulfatih 1981). The characteristic of the study area represents a degraded landform, and the socio-economic activities revolve around utilization of natural resources that need immediate attention in terms of conservation and development. The geophysical characteristics of the watershed distinguish the study area to demonstrate the applicability of the methodology.

Data and methods

The present study shows the application of various data sources to be used in landslide susceptibility evaluation. To evaluate the landslide susceptibility mapping (LSM), it is essential to know the preparatory and trigging factors and to prepare the necessary thematic layers. For this purpose, eleven thematic maps, viz. slope, rainfall, aspect, geomorphology, geology, soil erodibility, elevation, land use/land cover (LULC), drainage, lineament, the proximity of the road, generated using remote sensing (RS) and conventional data with the help of ArcGIS 10.3. All the spatial data were geometrically rectified to a common Universal Transverse Mercator (UTM-WGS84) coordinate system and resampled to their respective spatial resolution using the nearest-neighbour algorithm. The details of the data collection procedure, preparing the inventory map, landslide conditioning factors, and model building and validation described as follows:

Data collection

Data collection includes data sources and data types used in the present study.

Field survey, a reconnaissance survey was carried out at different times during October–November months was done to identify the various land use/land cover classes, soil sampling for grain size (texture) analysis present in the study area and existing landslide site. Other data sources such as historical landslide events (collected from the transportation authority, published articles, i.e. newspaper, and interaction with local people) can give some ideas about the frequency of landslide events. *Satellite images*, Landsat-8 with a spatial resolution of 15 m, worldview-2 with spatial resolution 0.5 m, and ALOS PALSAR Radiometrically Terrain Corrected (RTC) DEM with 12.5-m resolution. *Experimental data*, the collected soil samples analysed in the laboratory for soil properties, i.e. sand, silt, clay, organic content, and density. *Meteorological data*, the historical records of rainfall data (from 8 rain gauges stations) that located in and around the watershed used. *Geological data*, geological maps from the 1:250,000 Abha quadrangle GM-75 digitized.

Preparation of landslide inventory map

Preparation of inventory maps is a crucial part of landslide hazard analysis (Guzzetti et al. 2006), for example, the spatial distribution of landslides susceptibility (Pradhan and Lee 2010; Pourghasemi et al. 2012). A landslide inventory map describes the location, i.e. landslides are more likely to be trigger under the same conditions that had been found on earlier landslide, numbers and other data of occurrence and the types of mass movements that have left discernable traces in an area (Guzzetti et al. 2012). A landslide inventory map was prepared according to the interpretation of different data such as historical landslide events, field investigations, interaction with local people about the landslide events and satellite images analysis (Van Westen et al. 2006). Historical landslides have some significant geomorphological features that easily identifiable with high resolution (worldview-2), especially in the 3D models, including decreases in the densely vegetated area and bare soil (Mallick et al. 2014). Other notable features that may assist in detecting landslide area include the presence of flow materials along gullies, rims, and drainage networks with different erosional features and sedimentation (Mallick et al. 2014). Field survey and observations were conducted to verify and collect some recent landslides in the study area (Fig. 2). These all data were collected and combined to prepare the landslide inventory map. Using data sources (local government agencies, remote sensing data (LANDSAT 8 image), high resolution satellite images (Google Earth RS image), and ALOS PALSAR DEM (12.5 m), topographic map (scale 1:25,000), and verified using intensive field investigation, a total of 38 landslides identified and mapped in the study area, among them about 17 landslides visited in the field for verification purposes. Results depicted that all these locations are new and old landslide area, characterized by different intensity (volume) ranging from a few to thousand cubic metres. These landslide sites refer mainly translational slide mass movements (landslide is a downslope movement of material that occurs to a distinctive surface of weakness such as a fault, joint or bedding plane). It occurs mainly along the structures; another type of landslide is rotational slides, it occurs mainly in the highly fractured rocks and wadis terraces. Predominantly landslides were identified along the faults (lineaments). Geological structures, such as cleavage (rock to split on a set of regular parallel or subparallel planes), schistosity (orientation of equant minerals in a rock), fractures and joints, with a dip angle of more than 30° towards the wadis facilitate many planer failures.

Landslide sites were identified and collected (GPS) and digitized as point features. In GIS, point data can be expressed as *X, Y* coordinate (UTM-WGS84), does not depict landslide occurred areas. Therefore, point data may be considered when the areal extent of a minor landslide cannot be drawn because of the scale of the map (Yilmaz 2009). However, the logical method is to reveal the pixel belonging to the landslide. For the map of scale 1:5000–1:50,000, the 5-, 10-, 30-m pixel sizes yield similar accuracy (Lee et al. 2004a, b). In the present study, landslides larger than one pixel (12.5 × 12.5 m) were used in the analyses.

Landslide causative factors: generation of thematic maps

The landslide susceptibility map is generated based on identified criteria (thematic features related to the causative factor) that are relevant to the concerned environment and geophysical conditions. The set of criteria selected should adequately represent the landslide occurrence and should contribute towards the study objective (Feizizadeh and Blaschke 2013). The selected set of criteria should address the landslide and also fulfil the objectives of the research. In the present study, the boundary of the watershed was delineated using digital elevation model (DEM) of 12.5-m pixel resolution. Eleven causative factors identified for landslide susceptibility mapping. These include slope aspect, slope, rainfall, geology, geomorphology, distance from lineament, distance from drainage networks, distance from the road, land use/land cover, soil erodibility and vegetation proportion. All the thematic layers were transformed into a raster spatial database by 12.5 × 12.5 m pixel size using a nearest-neighbour algorithm with the projection system, UTM coordinate system zone 38 N, datum WGS84. Out of 11 thematic layers, three layers (slope angle (Lee and Min 2001), slope aspect (Yalcin et al. 2011) and drainage network (Tarboton et al. 1991) were extracted from digital elevation model (DEM) using ArcGIS 10.3 software.

Fig. 2 Field survey

The slope angle is one of the important aspects in landslide susceptibility analysis. The relationship between landslide occurrence and slope angle emphasizes the role that landslides have in landscape evolution. Usually, slope steepness is significantly triggered by the geological characteristics of the slope. Initially, slope failure began at the foot of homogeneous slopes, leading to the location where the stresses were the highest. Slope failure began with disintegration of the slope material by the breakage of interparticle bonds, leading to loss of cohesion. After that, failure spread upward to an upper part of the slope or to the slope crest (Katz et al. 2014). Finally, slope material overlying the sliding surface slides down the slope, runs out for some distance, and finally deposits downslope. The slope angle and slope aspect was derived from 12.5 m × 12.5 m pixel size ALOS PALSAR DEM data of the Abha watershed using

ArcHydro tools of ArcGIS software. The slope angle ranges from 0° to 52.32°. The western and north-western part of the study area comprises of a high degree of slope, whereas the central-south and eastern parts of the watershed consist of the low degree of slope. From the results, it inferred that high slope (20°–30°) with overlay rainfall renders the area highly susceptible to landslide (Yalcin and Bulut 2007). Figure 3a–d shows the elevation, slope angle, drainage networks and slope aspect (Fig. 3d). The occurrence of landslides is likely affected by topography (elevation), and this topography is controlled by several hydrogeologies, geomorphological processes (i.e. geological types, precipitation, temperature, and soil erosions) (Pourghasemi et al. 2013).

Visual image interpretation techniques using Landsat-8 satellite data and expert knowledge (geomorphologist) have been used to create the geomorphological map as per
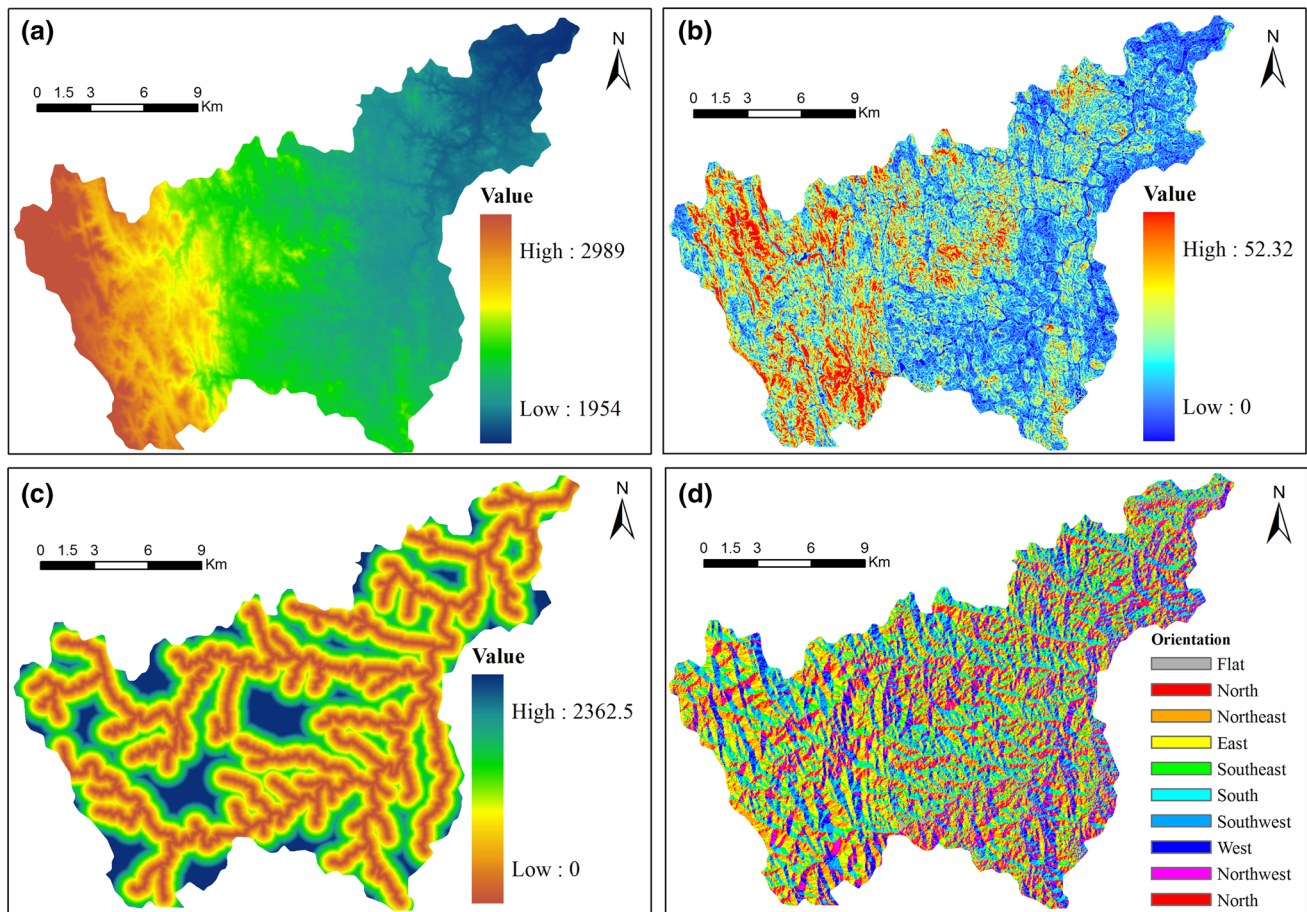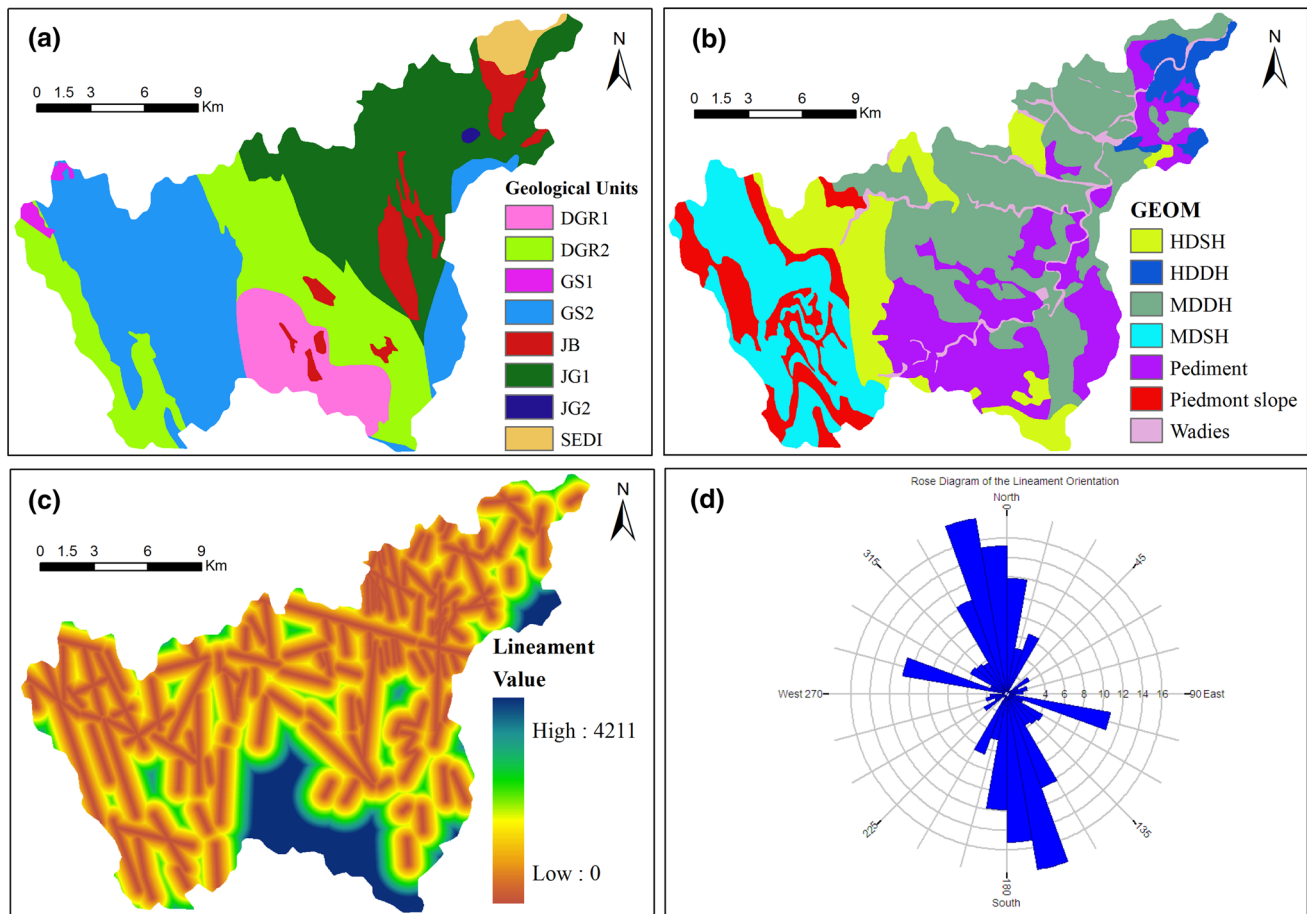
Fig. 3 Spatial distribution of the selected criteria: **a** DEM, **b** slope, **c** distance to drainage, and **d** aspect

the standards from the National Research Council (NRC) program, Geological Survey of India (The National Geomorphological and Lineament Mapping-NGLM) manual (GSI and NRSC 2010). The seven geomorphological units were extracted using visual image interpretation techniques including wadies, Piedmont slope, moderate-dissected denudational hills (MDDH), highly dissected structural hills (HDSH), pediment, highly dissected denudational hills (HDDH), and moderate-dissected structural hills (MDSH) (Fig. 4b). The catchment geomorphology plays a vital role in the conversion of rainfall into a runoff (Singh et al. 2014) and has been considered as a dominant factor in triggering a landslide (Cardinali et al. 2002). A large part of the watershed is covered with piedmont slope and the low-dissected structural hill which considered as high susceptible landslide occurrence. The flow direction of major wadies from North-West to South-East direction. The pediment is a gradually inclined erosional surface sliced in hard rock, i.e. exposed granite rock, thinly veneered with gravel, which is developed at the foothills, has considered moderate susceptible for a landslide. Highly denudational hills and highly dissected structural hills, having eroded structures, formed as a result

of differential erosion and weathering. These occupy the west and north-eastern parts of the area. It has the potential for a landslide trigger. Highly structural hills are the acute and linear hills exhibiting definite trend lines with varying lithology associated with faulting and so on and mostly act as susceptible landslide zone.

Geological map (Hardcopy format) collected from the Saudi Geological Survey at a scale of 1:250 000 Abha quadrangle GM-75 (Greenwood 1985). The hard copy map first scanned, geometrically rectified and then the heads-up digitizing procedure to a prepared thematic layer of geology. Figure 4a shows details of geology classes that are mainly underlined by Dioritic and Gabbroic rocks layered sills, dikes etc., sedimentary sandstone; volcanoclastic, shale and siltstone; basalt, andesite and carbonaceous conglomeratic; and granite suite. The dominant group of rocks such as volcanoclastic, shale and siltstone are covering significant parts of the study area. Small extent of sedimentary sandstone, which is highly permeable and less stable, is identified in north-western part of the study area. Besides that, Dioritic and Gabbroic rocks layered sills, dikes etc., which is considered as low hazard zones due to moderate denudational and

Fig. 4 Spatial distribution of the selected criteria: **a** geology, **b** geomorphology, **c** distance from lineament, and **d** lineament rose diagram. Details related to the abbreviation used for geomorphological unit (4B): HDSH = fighly-dissected structural hills; HDDH = highly dissected denudational hills; MDDH = moderate-dissected denudational hills; and MDSH = moderate dissected structural hills

dissected structural hills situated in the north-east parts of the watershed. However, basalt, andesite and carbonaceous conglomeratic; granite suite and quartzite are the hard rock materials located mainly in the central-south, eastern and north-eastern parts of the study area and considered for high landslide potential areas due to high potential for runoff.

These geological data and structural data verified during the field. Various type of information was collected through on site investigation and available literature (Youssef et al. 2015a, b). During site investigation, the joint planes and minor faults were identified. All landslides, in the study identified and mapped using remote sensing data (LANDSAT 8 image), high resolution satellite images (Google Earth RS image), and ALOS PALSAR DEM (12.5 m), topographic map (scale 1:25,000), and verified using intensive sites investigation. The area is commonly prone to landslide activities (rock falls, sliding, and debris flows) and erosion due to runoff through different gullies. The study area is traversed by many faults where several shear zones are situated. These tectonic features, in the studied watershed region,

are responsible for crushing and shearing of the rockmass. According to geological map (Abha quadrangle GM-75), the study area and its surroundings comprise of faults and linear structures (Greenwood 1985). These faults and linear structures were verified by field investigation. Major fault that cut through the rocks were noticed along the main curvature of the study area. These fault zone's materials are highly crashed and weathered along the gullies. The study area is significantly affected by faults and the rock characteristics in the most of the area are highly jointed and mixed together along with many colluvium soils are located with different sizes where shallow debris overburden extending below the homogenous slope (Youssef et al. 2015a, b). The unconsolidated overburden materials, when saturated during rains, form debris flows. These sliding blocks and the debris flows are affected the human lives, destruction of houses and facilities, and damage to the environment. It is also noticed that the Geological structures, such as cleavage (rock to split on a set of regular parallel or subparallel planes), schistosity (orientation of equant minerals in a rock), fractures and

joints, with a dip angle of more than 30° towards the wadis facilitate many planer failures.

The lineaments demonstrate the zone of weakness surface proving some linear to curvilinear features such as fracture, joint, fault in the geological structure (Mandal and Maiti 2014). Landsat-8 satellite imagery and geological map (Abha quadrangle GM-75) have been used to prepare the lineament map. The visual interpretation techniques carried out to identify the lineaments by using False Color Composite (FCC) of satellite data (band 4, band 7 and band 1) (Suzan and Toprak 1998), as per the literature band 4 was found to be the good in depicting the textural features (Pradeep et al. 2000) for lineament interpretation. After that, the visual interpretation enhanced by considering a 99% linear contrast stretch (more details could be found in Arlegui and Soriano 1998). After that, distance map prepared for lineament using Euclidean distance tool in ArcGIS 10.3 (Nalbant and Alptekin 1995). Rose diagram has been constructed to analyse the orientations of the lineaments. The density of lineament is high in the west and north part of the study area (Fig. 4c). This diagram indicates the high occurrence of the lineament towards N 330°–360° and S 165°–180°. The dominant trends of the lineament are found along the NNW-SSE and WNW-ESE (Fig. 4d). In this study, we considered that the distance of 150 m from lineament is dominated by a high percentage of the landslide (Mandal and Maiti 2014). The Euclidean distance tool of ArcGIS was also used for preparing the distance maps for drainage networks and roads. The maps show the distance from lineaments ranges from 0 to 4211 m, distance from roads ranges from 0 to 2070 m, and distance from drainage network ranges from 0 to 2360 m.

Rainfall is one of the most important climatic variables that essentially prerequisite for various applications including landslide susceptibility modelling (Xu 2015). Therefore, it is essential to understand its temporal and spatial phenomena required for hazard-related studies. Rainfall data for the last 30 years (during the year of 1986–2016) collected from Presidency of Meteorology and Environment (PME), Saudi Arabia of eight (8) rain gauges stations, which distributed over and nearby the studied area. In our methodology, we used long-term precipitation for a 30-year period. An average annual rainfall is mapped out from the daily rainfall data measurements (Duman et al. 2005; Shahabi and Hashim 2015; Feizizadeh et al. 2014). The rainfall data were interpolated using the geostatistical technique, i.e. inverse distance weighted (IDW) method (Lu and Wong 2008) in the ArcGIS platform to analyse the spatial variability of rainfall. Analysed data show that the maximum annual rainfall data (30 years) were ranging from 118 mm to 342 mm, with the average annual value of 215 mm (Fig. 5a) of the study area. The spatial distribution of rainfall and its occurrences mostly depends on climatic and topographical factors. In the mountainous regions, the elevation factor is a key factor affecting the rainfall (Berhanu et al. 2013).

For the most part, anthropogenic activities are to blame for deforestation, high sedimentation rate, high runoff, loss in soil quality, and triggering forces of global and regional climate change (Dwivedi et al. 2005; Mallick et al. 2014). The land use and land cover (LULC) are one of the critical factor responsible for landslide occurrence due to the transformation of natural surfaces. Landsat-8 satellite datasets of October 2014 was used to produce the LULC map using supervized classification (Nicholas 2005 (maximum likelihood classifier). The validation of the classification result is performed using confusion or error matrix (Lillesand and Kiefer 1999), and it found with good agreement. The major LULC class (Fig. 5b) was found in exposed rock, followed by scrubland, sparse vegetation, and built-up area. Rock exposed areas and bare soil have high susceptible to landslide (Feizizadeh et al. 2014).

Vegetation in a semi-arid climate characterized by heterogeneous landscape patterns of bare land and green areas. It is well known that vegetation can play a significant role in slope stability through hydrological and mechanical processes; these impacts can be adverse or beneficial to stability. The characteristics of the bare lands are usually formed by exposed rock and crusted soils with low soil structure, low depth and low infiltration rates. This makes overland flow highly discontinuous with bare land areas as runoff generating areas. However, in the vegetated areas have considerably better soil properties such as high organic matter content and a stronger aggregation, thereby, results in a higher infiltration capacity and areas as runoff sinks (Cammeraat and Imeson 1999). The amount and type of vegetation on a site will also play an essential role in landslide susceptibility. Vegetated branches assist in slow down water that flows over the soil surface, and it also consolidates the soil in place, whereas in the absence of the vegetated branches or root systems of trees, bushes, and other plants, the land surface is more likely to slide away.

In the present study, the vegetation proportion cover per pixel level is calculated from Landsat-8 satellite datasets using equation mentioned in Valor and Caselles (1996). Analysis of vegetation proportion shows that the value ranges from 0.00 to 1.00 with a mean of 0.12 (Fig. 5c). The highest patch of vegetation proportions located over the north-western part and along the wadies whereas lowest towards the east part of the study area. In this study, the highest value of vegetation proportion covers considered as low landslide susceptibility, whereas the lower values considered for high landslide susceptibility.

Soil samples collected from the study area during dry weather conditions using stratified technique, i.e. an area classified into similar topography, soil moisture and land cover, were determined using a Global Positioning System
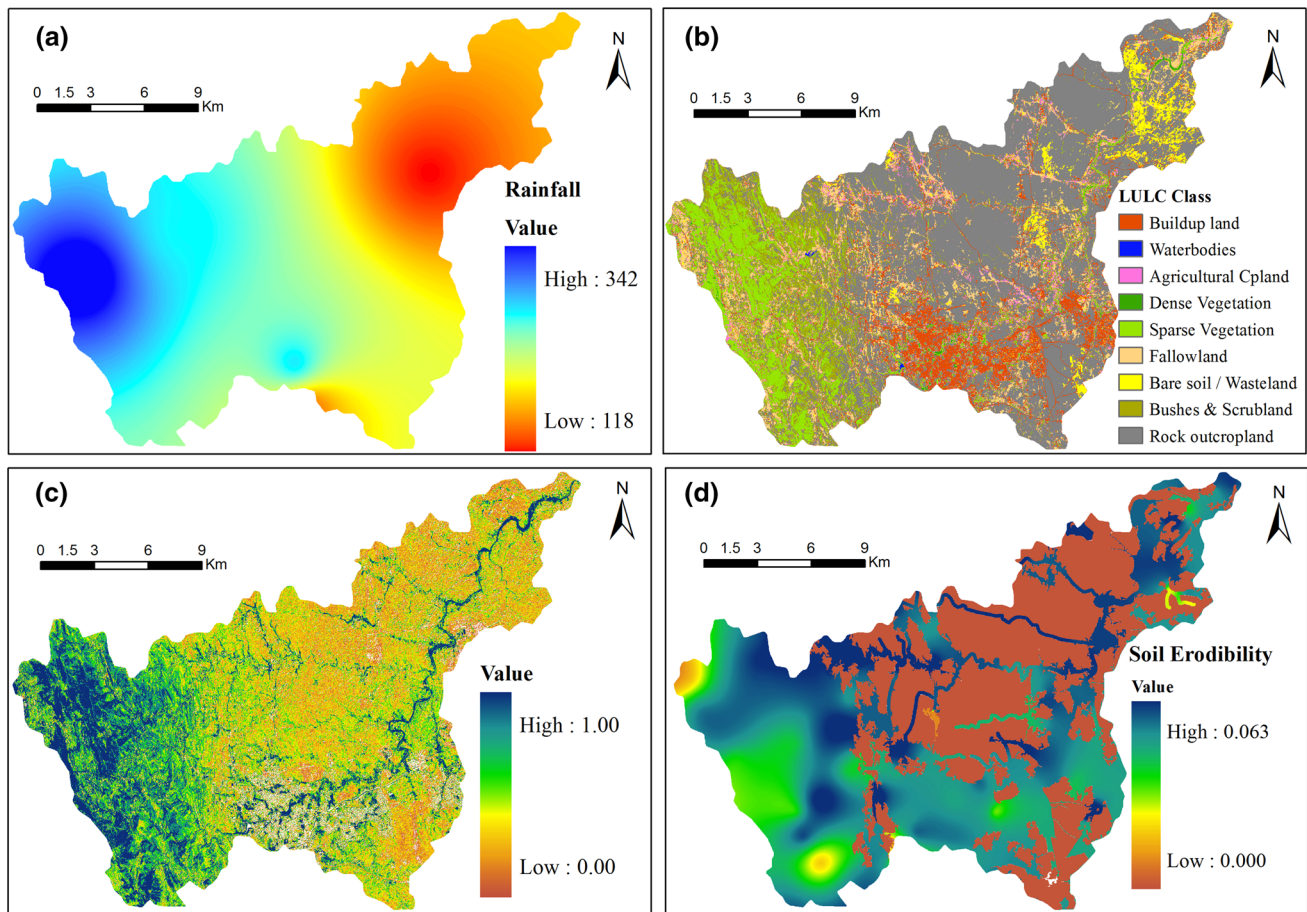
Fig. 5 Spatial distribution of the selected criteria: **a** rainfall, **b** land use/land cover, **c** vegetation proportion, and **d** soil erodibility

(GPS) model GPS 38S. A total of seventy-five (75) soils sample were collected from each site with two replicates each 2–3 m apart at the depth of 0–30 cm. In the laboratory, after air-drying (102 °C for 24 h in oven), soil samples crushed and pass a 2-mm sieve and carefully homogenized and later analysed in laboratory for their properties, namely soil texture, and organic matter content, using standard procedure described by Carter (1993). Organic matter content obtained from high temperature of 350–600 °C for 2 h using muffle furnace. The precision of the measurements is specified to 1.5% of the detected amount, with a detection limit of 0.02% (Hill and Schutt 2000). Texture analysis of the soil samples was done by hydrometer method using stokes' law (Sheldrick and Wang 1993). The grain size (sand, silt and clay %) and organic matter content % were analysed in order to estimate the soil erodibility.

The soil erodibility factor "K" characterizes the average long-term soil and soil-profile response to the erosive power related to rainfall and runoff. Soil erodibility factor is one of the essential factors required in the landslide studies (Lee 2004), and integrated watershed management (Mallick 2016). The soil erodibility factor is influenced by the detachability

of the soil, by infiltration and runoff, and the transportability of the sediment eroded from the soil. The key soil properties affecting K are soil texture (sand, silt, and clay percentages used to describe soil texture), organic matter, soil structure, and the permeability of the soil profile (Renard et al. 1997). K factor has been calculated using equation no. 1 (Wischmeier and Smith (1978)

$$K = 0.0293(0.65 - D_G + 0.24D_G^2)$$

$$\exp\left\{-0.0021\left(\frac{OM}{f_{clay}}\right) - 0.00037\left(\frac{OM}{f_{clay}}\right)^2 - 4.02f_{clay} + 1.72f_{clay}^2\right\}$$

$$(1)$$

where the geometric mean of soil particle size, and K factor unit is in (ton ha h ha^{-1} MJ^{-1} mm^{-1}), OM is percentage of organic matter contents, f_{sand} is the sand % (particle size of 0.05–2.0 mm), f_{silt} is the silt % (particle size 0.002–0.05 mm), f_{clay} is the clay % (particle size less than 0.002 mm) as per guideline USGS.

$$D_G = -3.5f_{clay} - 2.0f_{silt} - 0.5f_{sand} \qquad (2)$$

Result depicts that the K factor ranges from 0.000 to 0.0627 ton ha h ha^{-1} MJ^{-1} mm^{-1}, with an average value

and standard deviation of 0.043 and 0.0147, respectively. It observed from the generated map (Fig. 5d) that the high values of K factor mainly located in the north-western and west-eastern part of the study area. As per the outcomes of the result, it has been inferred that susceptibility of landslide is high where the soil erodibility is maximum, due to soil particle size either above or below the range of 20–200 μm, above this range it is more difficult to detach particles because of the mass and below this range cohesive forces counter particle detachment (Carlos and Odette 2012). Hence area with light texture soil (i.e. silt) and low organic matter content had the highest K values due to that the detachment increases as soil particles size are in the range of 20–200 μm (Mallick 2016).

Selection of thematic layers

In the recent past related to GIS-based landslide studies, it is inferred that the selecting of the various thematic maps having a significant role in the landslide susceptibility mapping (Pourghasemi et al. 2013). Such a bias approach of selecting the thematic layers for landslide susceptibility mapping may produce incorrect results. In this study, multivariate techniques, viz. Principal Component Analysis (PCA) (Jensen 2005) and expert opinions considered for assigning weights and normalization (from various stakeholders such as geologist, geotechnical experts, and local government bodies) were implemented to provide more robustness to the final result of a landslide susceptibility mapping. PCA is a statistical tool that uses an orthogonal transformation to convert a set of observations of possibly correlated criteria (or thematic maps) into a set of values of linearly uncorrelated variables. This leads to discriminate the groups of statistical values that could have a potential relationship (Jensen 2005). Principal components with more than 60% variance can be taken into account (Andreo et al. 2008) for statistical study. In the present study, PCA was performed for the eleven criteria.

Fuzzy set theory in multi-criteria decision-making

Zadeh (1965) first introduced the fuzzy set theory is modelling approach which simulates the complex systems that are difficult to explain by crisp numbers. Fuzzy logic allows the input of ambiguous, imprecise, and vague information (Balezentiene et al. 2013). Fuzzy logic is usually used in decision-making to carry out the spatial object on a map as a fuzzy membership function. In the case of classical set theory, a crisp number of an object either belongs to a particular set or not. However, in fuzzy set theory, the objects can belong as a membership value that ranges between 0 and 1 which shows the degree of membership function (Zadeh

1965). Figure 6 shows an example of a triangular fuzzy number (TFN) $\tilde{M}$.

A triangular fuzzy number (TFN) signified as (*l/m, m/u*) or (*l, m, u*) represents the smallest possible value, the most likely value and the most significant possible value, respectively. The TFN having linear representation on left and right side can be referred in term of its membership function as:

$$\mu\left(x\backslash\tilde{M}\right) = \begin{cases} 0, & x < l, \\ (x-l)/m-l), & l \le x \le m \\ (u-x)/(u-m), & m \le x \le u \\ 0, & x > u \end{cases} \tag{3}$$

A fuzzy number with its corresponding left and right representation of each degree of membership is as below (Kahraman et al. 2003):

$$\tilde{M} = \left(M^{l(y)}, M^{r(y)}\right) = (l + m - l)y, u + (m - u)y) \tag{4}$$

where $l(y)$ and $l(r)$ refers the left side and the right side representation of a fuzzy number, respectively

Fuzzy membership function (FMF)

The significant role of fuzzy set theory and fuzzy membership functions (FMF) can represent the vague data. It also permits mathematical functions and programming to use in the fuzzy domain. A fuzzy set is a class of objects characterized by a membership function, which assigns each object a grade of membership between 0 to 1 and vice versa (Zadeh 1965). In the case of landslide susceptibility mapping, the concept of partial membership of a considered location for more than one susceptibility class is possible by fuzzy sets theory. In this context, fuzzy membership's functions were assigned to analyse the spatial variability and its pattern that resulted in the development of continuing class boundaries for each hazard zone. The transition between 0 and 1 which takes place can be determined by the shape of each applied FMF.
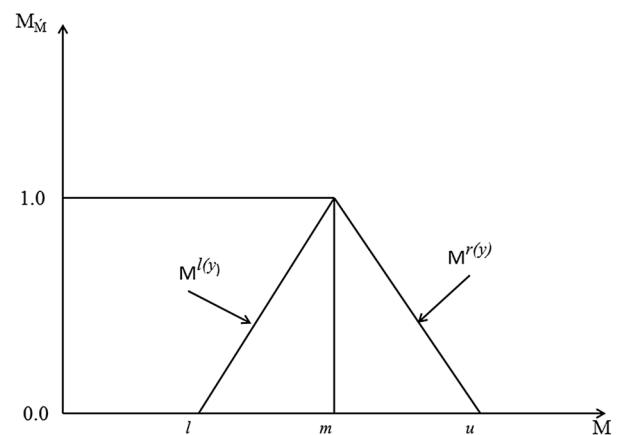

Fig. 6 A triangular fuzzy number (TFN) $\tilde{M}$

Thematic data standardization using FMFs

The thematic layers (criteria) for landslide susceptibility mapping generated in different units as well as levels of measurement. The four levels of measurement defined as nominal, ordinal, interval, and ratio (Akgun and Türk 2010), which necessitates the need for data standardization. Hence, the evaluation process requires incorporating all susceptibility triggering criteria into one output. So, the fuzzy membership approach adopted standardization methods (Liu 2004). The use of fuzzy sets theory in geospatial-based hazard and landslide assessment has been considered as an improved result (Mason and Rosenbaum 2002). Therefore, all the landslide triggering factors were standardized in range of 0 (low susceptible) to 1 (high susceptible). As per the objectives and problem definition we have used three membership functions for landslide susceptibility such as linear FMFs (A linear increasing or decreasing membership between tow inputs: linearized sigmoid shape), large FMFs (Sigmoid shape where large inputs have large memberships) and categorical FMFs (each named class assigned a membership value by the expert) (see Fig. 7). The first two sigmoidal membership function used commonly in many fuzzy logic applications and provided a gradual variation from non-membership (0) to complete membership (1) (Akgun and Türk 2010), although it is sometimes inevitable to select user-defined FMFs or categorical membership functions. Figure 7 represents FAHP-based membership functions including: (Type I) large for (a) rainfall, (Type II) linear FMFs for (b) Soil erodibility c) distance to roads, (d) distance to lineament, (e) distance to drainage, (f) vegetation proportion, and (Type III) categorical FMFs for (g) slope (h) aspect (i) geomorphology (j) geology and (k) land use/cover. All applied FMFs of criteria and the subsequent output raster maps are shown in Figs. 7 and 8, respectively.

Assignment of weights and normalization

The expert's opinions are considered for assigning suitable weights and its normalization. Assignment of weights has been recommended by Saaty (1980) but it was not significantly considered in the earlier studies. Analytical Hierarchy Process (AHP) has been extensively used in multi-criteria decision analysis (MCDA) to obtain the appropriate weights for different criteria (Saaty 1977; Ohta et al. 2007). It has been successfully implemented in GIS-based MCDA studies (Carver 1991; Malczewski 1999, 2004; Marinoni et al. 2009). An AHP calculates the required weights associated with the relevant thematic layers assist with the opted matrix in which all the identified criteria (thematic layers) are compared and analysed with each other (Feizizadeh and Blaschke 2013; Mallick 2016). The weights combined with values (criterion) generate a single-scale value for particular decision variant (spatially), which shows the relative importance of the value concerned. Since, the conventional

AHP cannot appropriately depict the decision-making process based on the quantitative articulation of preferences, a fuzzy extension of AHP (called FAHP) was evolved to solve the fuzzy hierarchical problems. In the present study, the FAHP approach implemented for hierarchical analysis fuzzification by assigning fuzzy numbers for the pairwise comparisons, to obtain fuzzy weights. To determine evaluation criteria, weights for FAHP following steps were adopted (Chen et al. 2011).

Step I: Pairwise comparison matrices were established using all the elements/criteria in the dimensions of the hierarchy system. Linguistic terms were assigned to the pairwise comparisons as follows, asking in each case, which of the two elements/criteria were more important:

$$\tilde{A} = \begin{bmatrix} \tilde{1} & \tilde{a}_{12} & \cdots & \tilde{a}_{1n} \\ \tilde{a}_{21} & \tilde{1} & \cdots & \tilde{a}_{2n} \\ \vdots & \vdots & \ddots & \vdots \\ \tilde{a}_{n1} & a_{n2} & \cdots & \tilde{1} \end{bmatrix} = \begin{bmatrix} \tilde{1} & \tilde{a}_{12} & \cdots & \tilde{a}_{1n} \\ 1/\tilde{a}_{21} & \tilde{1} & \cdots & \tilde{a}_{2n} \\ \vdots & \vdots & \ddots & \vdots \\ 1/\tilde{a}_{n1} & 1/a_{n2} & \cdots & \tilde{1} \end{bmatrix} \quad (5)$$

where $\tilde{a}_{ij}$ measure denotes, let $\tilde{1}$ be $(1,1,1)$, when i equal j (i.e. $i = j$); if $\tilde{1}, \tilde{2}, \tilde{3}, \tilde{4}, \tilde{5}, \tilde{6}, \tilde{7}, \tilde{8}, \tilde{9}$ measure that criterion i is relatively important to criterion j and then $\tilde{1}^{-1}, \tilde{2}^{-1}, \tilde{3}^{-1}, \tilde{4}^{-1}, \tilde{5}^{-1}, \tilde{6}^{-1}, \tilde{7}^{-1}, \tilde{8}^{-1}, \tilde{9}^{-1}$ measure that criterion j is relatively important to criterion i (Table 1).

Step II: To use the geometric mean technique to define the fuzzy geometric mean and fuzzy weights of each criterion by Buckley (1985) as follows:

$$\tilde{r}_i = \left(\tilde{a}_{i1} \otimes \tilde{a}_{i2} \otimes \cdots \otimes \tilde{a}_{in} \right)^{1/n}$$
$$\text{And then} \quad \tilde{w}_i = \tilde{r}_i \otimes \left(\tilde{r}_i \otimes \cdots \otimes \tilde{r}_n \right)^{-1} \quad (6)$$

where $\tilde{a}_{in}$ is fuzzy comparison value of criterion i to criterion n, thus, $\tilde{r}_i$ is geometric mean of fuzzy comparison value of criterion i to each criterion, $\tilde{w}_i$ i is the fuzzy weight of the ith criterion, can be indicated by a TFN, $\tilde{w}_i = (lw_i, mw_i, uw_i)$. Here lw_i, mw_i, uw_i stand for the lower, middle and upper values of the fuzzy weight of the ith criterion, respectively.

Landslide susceptibility map

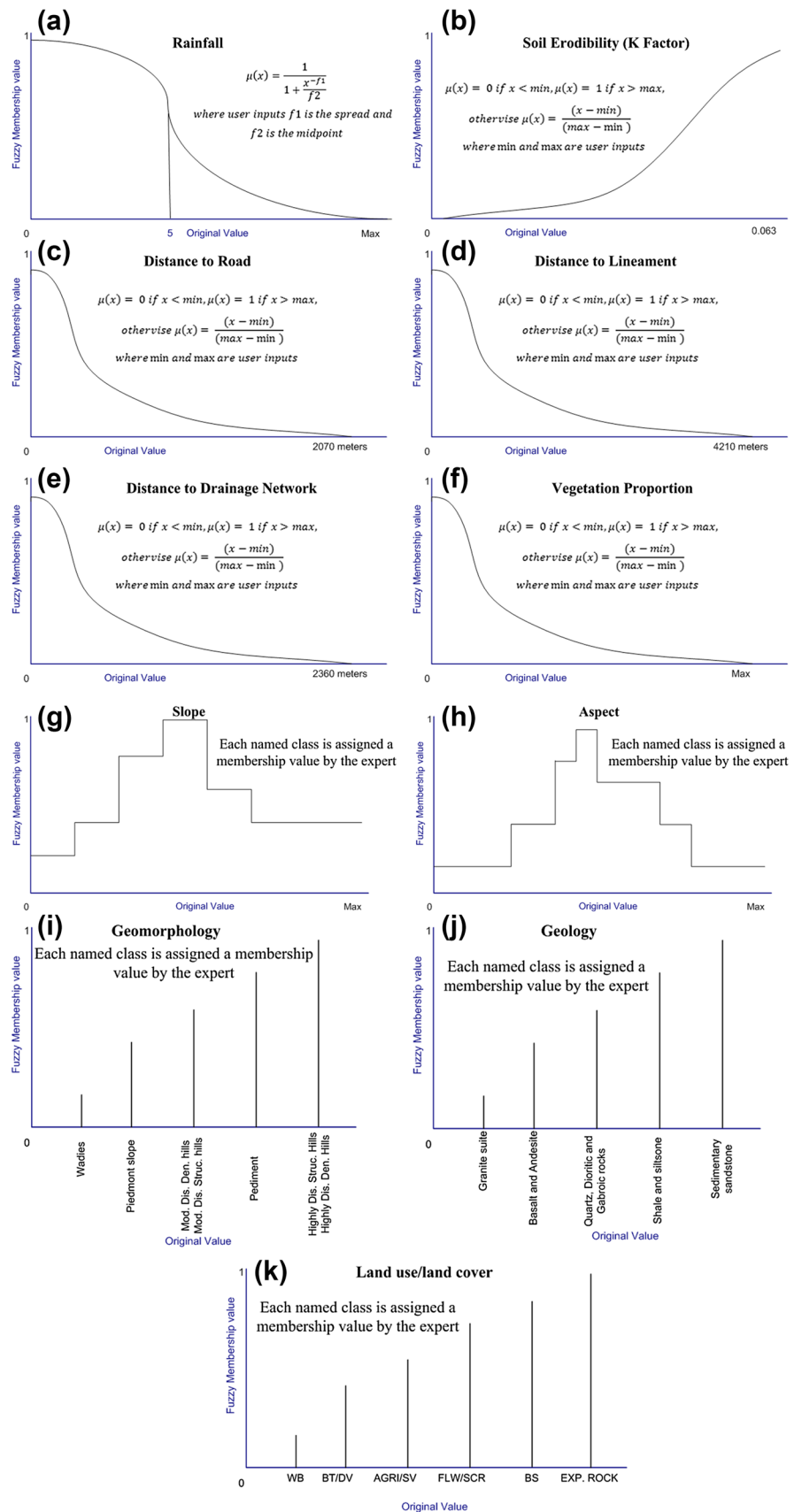The qualitative landslide susceptibility zone (LSZ) of the watershed obtained by integrating the thematic maps in the GIS environment. The weighted linear combination method used for the computation of the LSZ (Malczewski 1999) (Eq. 7):
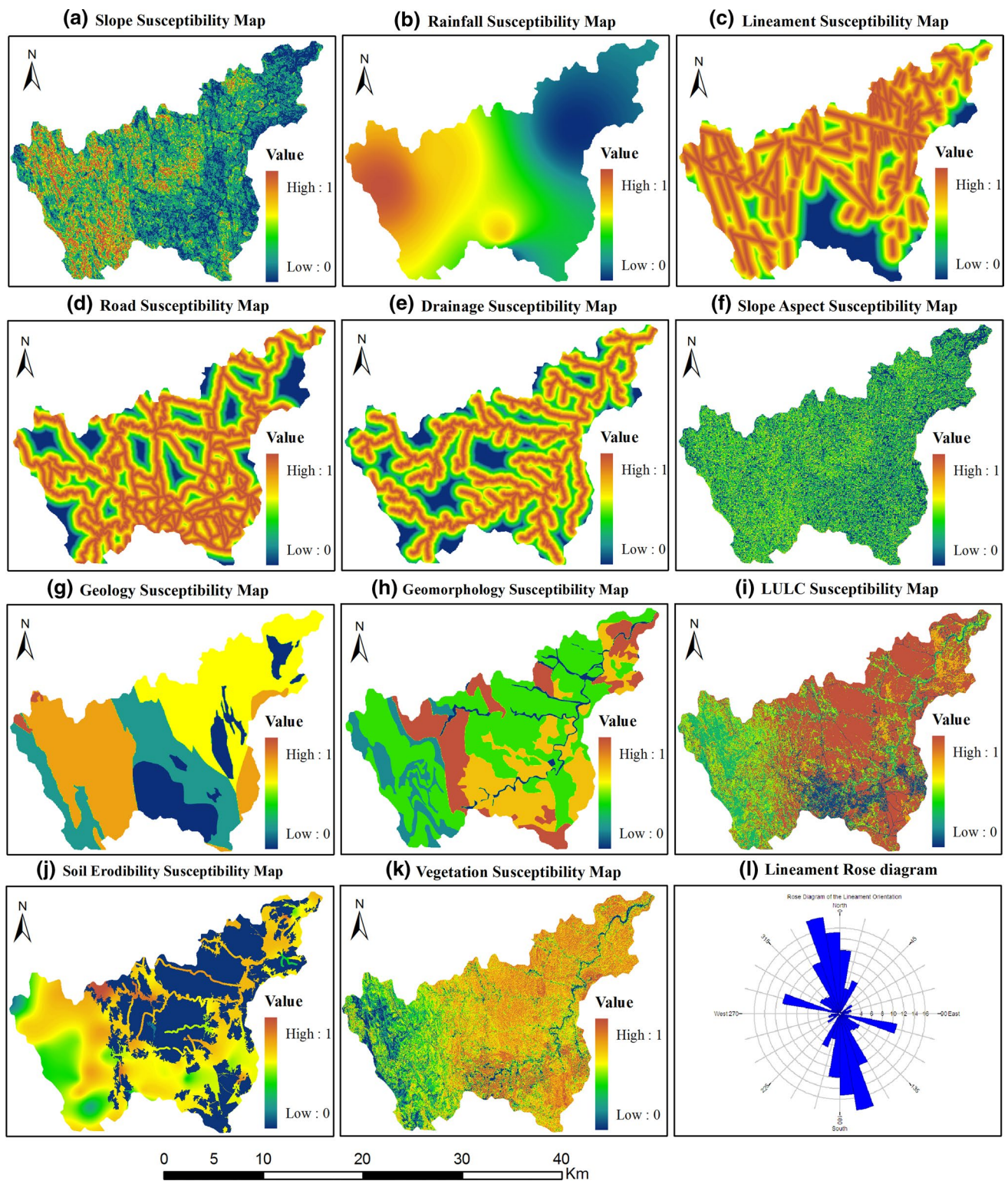
$$LSI = \sum_{w=1}^{m} \sum_{i=1}^{n} \left(w_j * x_i \right) \quad (7)$$

where LSI = landslide susceptibility index, x_i = normalized score (scale) of the ith class/feature of theme and

Fig. 7 FAHP-based membership functions including: (Type I) large for **a** rainfall, (Type II) linear FMFs for **b** soil erodibility, **c** distance to roads, **d** distance to lineament, **e** distance to drainage, **f** vegetation proportion, and (Type III) categorical FMFs for **g** slope, **h** aspect, **i** geomorphology, **j** geology and **k** land use/cover

(a) Rainfall

$$\mu(x) = \frac{1}{1 + \frac{x - f1}{f2}}$$

where user inputs $f1$ is the spread and $f2$ is the midpoint

(b) Soil Erodibility (K Factor)

$$\mu(x) = 0 \text{ if } x < min, \mu(x) = 1 \text{ if } x > max,$$
$$othervise\ \mu(x) = \frac{(x - min)}{(max - min)}$$

where min and max are user inputs

(c) Distance to Road

$$\mu(x) = 0 \text{ if } x < min, \mu(x) = 1 \text{ if } x > max,$$
$$othervise\ \mu(x) = \frac{(x - min)}{(max - min)}$$

where min and max are user inputs

(d) Distance to Lineament

$$\mu(x) = 0 \text{ if } x < min, \mu(x) = 1 \text{ if } x > max,$$
$$othervise\ \mu(x) = \frac{(x - min)}{(max - min)}$$

where min and max are user inputs

(e) Distance to Drainage Network

$$\mu(x) = 0 \text{ if } x < min, \mu(x) = 1 \text{ if } x > max,$$
$$othervise\ \mu(x) = \frac{(x - min)}{(max - min)}$$

where min and max are user inputs

(f) Vegetation Proportion

$$\mu(x) = 0 \text{ if } x < min, \mu(x) = 1 \text{ if } x > max,$$
$$othervise\ \mu(x) = \frac{(x - min)}{(max - min)}$$

where min and max are user inputs

(g) Slope

Each named class is assigned a membership value by the expert

(h) Aspect

Each named class is assigned a membership value by the expert

(i) Geomorphology

Each named class is assigned a membership value by the expert

(j) Geology

Each named class is assigned a membership value by the expert

(k) Land use/land cover

Each named class is assigned a membership value by the expert

Fig. 8 Spatial distribution of landslide susceptibility for each thematic layer, based on fuzzy membership functions (i.e. fuzzy or crisp) of each parameter: **a** slope, **b** rainfall, **c** distance to lineaments, **d** drainage to roads density, **e** distance to drainage, **f** slope aspect, **g** geology, **h** geomorphology, **i** land use/land cover, **j** soil erodibility and **k** land use/cover; and also show the **l** lineament orientation using rose diagram

Table 1 Fuzzy conversion scale

Importance intensity	Triangular fuzzy scale	Importance intensity	Triangular fuzzy scale
1	(1,1,1)	1/1	(1/1, 1/1, 1/1)
2	(1,2,4)	1/2	(1/4, 1/2, 1/1)
3	(1,3,5)	1/3	(1/5, 1/3, 1/1)
4	(2,4,6)	1/4	(1/6, 1/4, 1/2)
5	(3,5,7)	1/5	(1/7, 1/5, 1/3)
6	(4,6,8)	1/6	(1/8, 1/6, 1/4)
7	(5,7,9)	1/7	(1/9, 1/7, 1/5)
8	(6,8,10)	1/8	(1/10, 1/8, 1/6)
9	(7,9,11)	1/9	(1/11, 1/9, 1/7)

w_j = normalized weight of the jth theme, m = total number of themes, and n = total number of classes in a theme.

Sensitivity analysis

Sensitivity analysis is used to assess effects of the input criteria on the model output performance and also to validate the effect of changing variable conditions or parameter values on the system (Gomez and Jones 2010). The information on the effect of scaled values and weights assigned to each parameter verified by sensitivity analysis (Napolitano and Fabbri 1996). Therefore, the effective weights of each criterion compared with the assigned weight. The effective weight is computed using the following Eq. (8) (Napolitano and Fabbri 1996).

$$\text{Effective} \dots \text{weight} = \frac{\text{Theme}_w * \text{Theme}_s}{\text{LSI}} * 100 \qquad (8)$$

where w and s are, respectively, the weight and scaled value for the theme (Theme) assigned in each grid and LSI is the landslide potential index as computed from Eq. 7.

Results and discussion

The relationship between the detected landslide locations and eleven susceptibility factors identified by using GIS-based statistical models including fuzzy analytical hierarchy process (FAHP), weighted linear combination (WLC) and multi-criteria evaluation (MCE) technique. In the first stage, the theme standardization of landslide triggering criteria was performed after that the susceptibility map created by a GIS-based landslide susceptibility mapping technique. The selection of criteria, PCA loading help to interpret principal components. It is based on finding which variables are most strongly correlated linear combination weights (coefficients) with each component.

In this study, PCA loading reveals that all eleven sets of criteria are susceptible to landslide occurrence. The criteria weighting, typically, assign the attribute's weight was carried out using MCDA (multi-criteria decision analysis) techniques. Accordingly, slope, rainfall and distance form lineament is inferred as the most significant causative factor to the landslide occurrences. Apart from that the distance to the lineament, rainfall, distance to the drainage network and slope aspect criteria are also among the principal indexes of a landslide. The accuracy of predictive models ("what is likely to happen?") has played a significant concern in the majority of environmental modelling applications including hazard assessments.

The bias point of assessment from the decision maker for data standardization and criteria weighting affects the predictive accuracy. Moreover, the lack of synergy between expert opinions and stochastics model may cause limitation of the landslide susceptibility mapping process while using a subjective method. To preserve the quality of spatial data, more computationally intensive approach (FAHP and expert opinions) was considered for criteria standardization schemes. In this context, variety (linear, large and categorical) of fuzzy memberships functions (FMF) positively affected the validity and accuracy of input criteria. Further, the adopted methodology exhibits promising results to predict landslide occurrence irrespective of experts' opinion. Therefore, the efficiency of the proposed FAHP and MCDM model substantially improves the outcomes. The details of the results and discussions discussed below mentioned heads.

Identifying potential thematic layers for landslide susceptibility zone assessment

Table 2 shows the results of the Principal Component Analysis (PCA) including eleven PCs, eigenvalues, total variances and cumulative variances. PCA loading help to interpret principal components or factors; due to they are the linear combination weights (coefficients) whereby unit-scaled components or elements define or "load" a variable. The result infers that the first two principal components (PCs) explain about 80.27% of the total variance of the system. The plot of PC loading (Fig. 9) shows that all sets of variables are susceptible of landslide occurrence, while some the themes, such as vegetation proportion and land use/land cover are on the fourth quadrants, but they are very near to first positive quadrant of the axis. Hence, all variables may be contributing a significant role in landslide susceptibility occurrence. Thus, in this study, the landslide susceptibility zonation, all the eleven thematic layers were considered for proposed modelling.

Table 2 Principal component loadings of the 11 variables used in PCA

| Variable (themes) | Principal Component Analysis | | | | | | | | | | |
	Unit in NAW	I	II	III	IV	V	VI	VII	VIII	IX	X	XI
VG	0.0–1.0	0.28	−0.22	−0.09	0.05	−0.04	−0.14	−0.02	−0.51	0.21	0.47	0.21
Rainfall	0.0–1.0	0.32	0.20	0.16	−0.07	−0.06	0.10	0.21	0.42	0.00	0.40	0.59
DD	0.0–1.0	0.10	0.03	−0.33	0.18	0.62	0.08	−0.58	0.23	0.04	0.24	−0.02
DL	0.0–1.0	0.13	−0.06	0.10	−0.07	0.48	0.11	0.31	−0.44	−0.08	−0.10	0.09
DR	0.0–1.0	0.06	0.11	−0.35	0.24	0.37	−0.53	0.59	−0.05	−0.18	0.01	0.03
GEOM	0.0–1.0	0.39	0.54	0.28	−0.03	0.20	0.13	0.03	−0.01	−0.07	0.01	0.10
Geology	0.0–1.0	0.15	0.05	0.18	−0.07	0.07	0.14	0.33	0.29	0.30	0.44	−0.46
Slope	0.0–1.0	0.25	0.11	0.66	−0.23	0.34	−0.51	−0.19	−0.15	0.03	−0.05	0.00
LULC	0.0–1.0	0.41	−0.44	0.15	−0.04	0.25	−0.03	0.14	0.41	0.08	−0.11	0.09
SE	0.0–1.0	0.23	0.16	−0.08	0.04	0.09	0.03	0.09	0.20	0.40	−0.59	0.11
Aspect	0.0–1.0	0.23	0.27	0.38	0.21	−0.08	0.07	−0.02	−0.01	0.00	−0.01	−0.01
Eigenvalue	–	16.08	4.008	1.134	0.820	0.772	0.652	0.486	0.325	0.290	0.252	0.190
% of Variance	–	64.20	16.07	4.55	3.29	3.09	2.61	1.95	1.30	1.16	1.01	0.76
Cumulative Variance %	–	64.20	80.27	84.81	88.10	91.20	93.81	95.76	97.06	98.23	99.24	100.0
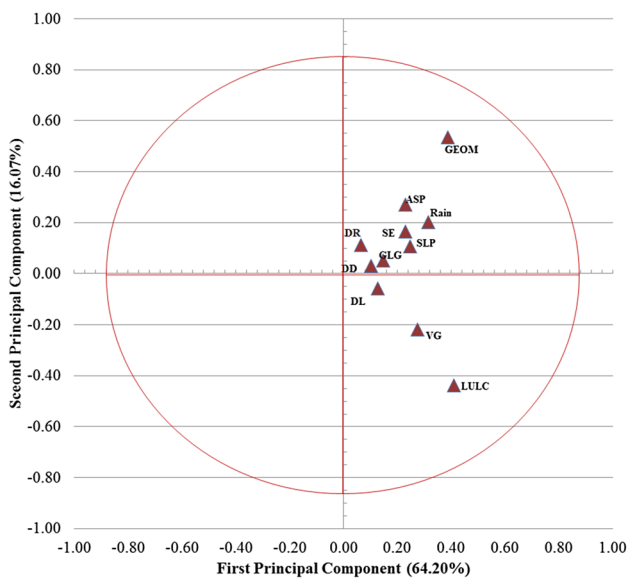
Fig. 9 Plot of loadings of first PC versus that of second PC for eleven thematic variables

Weights normalization for thematic maps

Table 3 summarizes the weights assigned to different thematic layers. The individual theme, as well as the classes of each thematic layer, normalized by the fuzzy analytical hierarchy process (FAHP) and eigenvector technique which is shown in Table 4. The statistical analysis such as consistency ratios (CRs) < 8%, eigenvector solution: 5–7 iterations, and delta = 5.1 E−8 to 6.7E−8 for assigned weights for the

eleven thematic layers and their features, shows that the assigned weights are consistent with the desired outcomes.

Validation of the results

Validation of the results by sensitivity analysis

The resulting outcome is verified by analysing the effective weight of a theme and compared it with the theoretical weight. Figure 10 represents the effective weights with the theoretical weight for each landslide susceptibility criterion. The effective weights for each theme are slightly different from the theoretical weight assigned to landslide susceptibility zonation.

Validation of the results using relative operating characteristics (ROC)

ROC curve analysis is generally utilized for evaluating the accuracy of a diagnostic test (Swets 1988, Williams et al. 1999). ROC curve is a plot of the probability of having a true positive (correctly predicted event response) on the X axis versus the probability of a false positive (falsely predicted event response) on the Y axis as the cut-off probability varies. For example, a true positive is a prediction of a landslide for an area where a landslide happaned, while a false positive is a prediction of a landslide for an area where a landslide did not happen (Nandi and Shakoor 2010; Roodposhti et al. 2014). The accuracy of the model can be measured by the area under ROC curve (Williams et al. 1999; Yilmaz 2009). An area of 1 shows a perfect test, while an area of 0.5 shows an insignificant test. The closer the curve follows the left-hand border and then the top border of the ROC space,

Table 3 Pairwise comparison matrix and normalized weights of the eleven themes

	SLP	Rainfall	DL	DR	DD	Aspect	Geology	Geom	SE	VP	LULC	Fuzzy weight
SLP	1,1,1	1,3,5	1,3,5	1,3,5	1,3,5	2,4,6	2,4,6	2,4,6	4,6,8	4,6,8	5,7,9	0.261
Rainfall	1/5,1/3,1/1	1,1,1,	1,3,5	1,3,5	1,3,5	2,4,6	2,4,6	3,5,7	4,6,8	4,6,8	4,6,8	0.178
DL	1/5,1/3,1/1	1/5,1/3,1/1	1,1,1,	1,3,5	1,3,5	1,3,5	1,3,5	2,4,6	3,5,7	4,6,8	5,7,9	0.128
DR	1/5,1/3,1/1	1/5,1/3,1/1	1/5,1/3,1/1	1,1,1,	1,3,5	1,3,5	1,3,5	1,3,5	3,5,7	5,7,9	5,7,9	0.103
DD	1/5,1/3,1/1	1/5,1/3,1/1	1/5,1/3,1/1	1/5,1/3,1/1	1,1,1,	1,3,5	1,3,5	1,3,5	2,4,6	4,6,8	5,7,9	0.085
Aspect	1/6,1/4,1/2	1/6,1/4,1/2	1/5,1/3,1/1	1/5,1/3,1/1	1/5,1/3,1/1	1,1,1,	1,3,5	1,3,5	3,5,7	4,6,8	4,6,8	0.064
Geology	1/6,1/4,1/2	1/6,1/4,1/2	1/5,1/3,1/1	1/5,1/3,1/1	1/5,1/3,1/1	1,1,1,	1,1,1,	1,3,5	2,4,6	3,5,7	4,6,8	0.056
Geom	1/6,1/4,1/2	1/7,1/5,1/3	1/6,1/4,1/2	1/5,1/3,1/1	1/5,1/3,1/1	1/5,1/3,1/1	1/5,1/3,1/1	1,1,1	1,3,5	1,2,4	2,4,6	0.044
SE	1/8,1/6,1/4	1/8,1/6,1/4	1/7,1/5,1/3	1/7,1/5,1/3	1/6,1/4,1/2	1/7,1/5,1/3	1/6,1/4,1/2	1/5,1/3,1/1	1,1,1,	1,2,4	1,3,5	0.029
VP	1/8,1/6,1/4	1/8,1/6,1/4	1/8,1/6,1/4	1/9,1/7,1/5	1/8,1/6,1/4	1/8,1/6,1/4	1/7,1/5,1/3	1/4,1/2,1/1	1/4,1/2,1/1	1,1,1,	1,1,1,	0.025
LULC	1/9,1/7,1/5	1/8,1/6,1/4	1/9,1/7,1/5	1/9,1/7,1/5	1/9,1/7,1/5	1/8,1/6,1/4	1/8,1/6,1/4	1/6,1/4,1/2	1/5,1/3,1/1	1/1,1,	1,1,1,	0.023

SLP slope, *DL* distance from lineament, *DR* distance from roads, *Geom* geomorphology, *SE* soil erodibility, *VP* vegetation proportion, *LULC* land use/land cover

the more accurate the test; the true positive rate is high and the false positive rate is low (Pradhan 2013; Roodposhti et al. 2014). The ROC method was executed based on the landslide inventory database. Accordingly, to compute the AUC, 38 known landslide sites chosen for the accuracy of the model and 31 non-landslides points (NLS points) randomly chosen within the bounds of the study area. Figure 11 shows the AUC of the ROC curve of 0.891 with a standard error of 0.038.

Validation of the results using simple overlay

The final landslide susceptibility map was also verified using the landslide inventory map. It has been carried out by overlaying the 38 known landslides sites on the landslide susceptibility map (see Fig. 12). About 73.68% of known landslides sites fell in the very high susceptibility and high susceptibility zones, while 15.79% accounts for moderate susceptibility and 10.53% belongs to low susceptibility category. No landslide event occurs in the "very low susceptibility" category.

Analysis of landslide susceptibility map

Results obtained from the study summarize the weighted overlay analysis method using MCDM (the FAHP and eigenvector techniques) is one of the reliable technologies to map landslide susceptibility zones. The eleven (11) thematic layers, slope, rainfall, distance to lineaments, distance to the road network, distance to drainage network, geology, geomorphology, slope aspect, soil erodibility, vegetation proportion and land use/land cover, to classify the studies study area into different landslide susceptibility zones. Figure 12 shows the landslide susceptibility map which was quantitatively developed using landslide susceptibility index (LSI) value for the interpretation. The mean value of the landslide susceptibility index was 16.92, and the standard deviation was 5.04, whereas the minimum and maximum values of LSI were 6.24 and 39.07, respectively.

Landslide susceptibility index classified into the various zone as per the histogram profile. The histogram profile displays the statistical information about pixel (cell) value of LSI that indicates the frequency of spread data. The histogram inferred that the spread values unevenly distributed, so natural-break classification scheme selected for zonation mapping (Constantin et al. 2011). Hence, the landslide susceptibility zones identified and mapped into five classes: very low susceptibility, low susceptibility, moderate susceptibility, high susceptibility and very high susceptibility (Fig. 12). As per the analysis, 5.59 and 9.53% of the total area of the study area were under very high and high susceptibility zone, while 22.55 and 35.58% were under the moderate and low susceptibility zone, respectively (Table 5). With this qualitative-based zonation, very high and high

Table 4 Assigned and normalized weights of different features of eleven thematic layers for landslide

| Theme	Feature classes	FMF	Assigned weight	Fuzzy weight
1. Slope in degree	a) Susceptibility class 1 (0.00–5.00 degree)	0.200	1	0.045
	b) Susceptibility class 2 (5.01–15.00 degree)	0.400	2	0.066
	c) Susceptibility class 3 (15.01–20.00 degree)	0.800	4	0.243
	d) Susceptibility class 4 (20.01–30.00 degree)	1.000	5	0.530
	e) Susceptibility class 5 (30.01–40.00 degree)	0.600	3	0.116
	f) Susceptibility class 6 (40.01–52.32 degree)	0.400	2	0.066
2. Rainfall	a) Susceptibility class 1 (118–155 mm)	0.000–0.123	1	0.039
	b) Susceptibility class 2 (156–183 mm)	0.124–0.242	2	0.050
	c) Susceptibility class 3 (184–211.mm)	0.243–0.397	3	0.068
	d) Susceptibility class 4 (212–236 mm)	0.398–0.532	4	0.098
	e) Susceptibility class 5 (237–259 mm)	0.533–0.644	5	0.149
	f) Susceptibility class 6 (260–290 mm)	0.645–0.760	6	0.222
	g) Susceptibility class 7 (291–342 mm)	0.760–1.000	7	0.374
3. Distance from lineaments	a) Susceptibility class 1 (2807–4211 m)	0.00–0.333	1	0.039
	b) Susceptibility class 2 (2097–2806 m)	0.334–0.501	2	0.050
	c) Susceptibility class 3 (1469–2096 m)	0.502–0.650	3	0.068
	d) Susceptibility class 4 (974–1468 m)	0.651–0.768	4	0.098
	e) Susceptibility class 5 (595–973 m)	0.769–0.858	5	0.149
	f) Susceptibility class 6 (280–594 m)	0.859–0.933	6	0.222
	g) Susceptibility class 7 (0–279 m)	0.934–1.000	7	0.374
4. Distance from roads	a) Susceptibility class 1 (1924–2870 m)	0.000–0.329	1	0.039
	b) Susceptibility class 2 (1384–1923 m)	0.330–0.517	2	0.050
	c) Susceptibility class 3 (1012–1383 m)	0.518–0.647	3	0.068
	d) Susceptibility class 4 (708–1011 m)	0.648–0.752	4	0.098
	e) Susceptibility class 5 (438–707 m)	0.753–0.847	5	0.149
	f) Susceptibility class 6 (203–437 m)	0.848–0.929	6	0.222
	g) Susceptibility class 7 (0–202 m)	0.930–1.000	7	0.374
5. Distance from drainage	a) Susceptibility class 1 (1510–2363 m)	0.000–0.360	1	0.039
	b) Susceptibility class 2 (1158–1509 m)	0.361–0.508	2	0.050
	c) Susceptibility class 3 (889–1157 m)	0.509–0.623	3	0.068
	d) Susceptibility class 4 (657–888 m)	0.624–0.721	4	0.098
	e) Susceptibility class 5 (436–656 m)	0.722–0.815	5	0.149
	f) Susceptibility class 6 (213–435 m)	0.816–0.909	6	0.222
	g) Susceptibility class 7 (0–212 m)	0.910–1.000	7	0.374
6. Aspect	a) Susceptibility class 1 (flat)	0.100	1	0.039
	b) Susceptibility class 2 (north)	0.200	2	0.056
	c) Susceptibility class 3 (north-east and north-west)	0.400	3	0.092
	d) Susceptibility class 4 (south and Southwest)	0.600	4	0.155
	e) Susceptibility class (east and Southeast)	0.800	5	0.238
	f) Susceptibility class (south-east)	1.000	6	0.42
7. Geology	a) Susceptibility class 1 (granite suite)	0.200	1	0.045
	b) Susceptibility class 2 (basalt, andesite and carbonaceous conglomeratic)	0.400	2	0.066
	c) Susceptibility class 3 (volcanoclastic, shale and siltstone)	0.600	3	0.116
	d) Susceptibility class 4 (dioritic and gabbroic massive layered sills, dikes etc.)	0.800	4	0.243
	e) Susceptibility class 5 (sedimentary–sandstone)	1.000	5	0.530

Table 4 (continued)

Theme	Feature classes	FMF	Assigned weight	Fuzzy weight
8. Geomorphology	a) Susceptibility class 1 (wadies)	0.200	1	0.045
	b) Susceptibility class 2 (Piedmont slope/Low-dissected structural Hills)	0.400	2	0.066
	c) Susceptibility class 3 (Moderate-dissected denudational hills/Moderate-dissected structural Hills)	0.600	3	0.116
	d) Susceptibility class 4 (Pediment)	0.800	4	0.243
	e) Susceptibility class 5 (highly dissected structural hills/highly dissected denudational hills)	1.000	5	0.530
9. Soil Erodibility	a) Susceptibility class 1 (0.000–0.010)	0.000–0.160	1	0.039
	b) Susceptibility class 2 (0.011–0.024)	0.161–0.388	2	0.056
	c) Susceptibility class 3 (0.025–0.033)	0.389–0.529	3	0.092
	d) Susceptibility class 4 (0.034–0.040)	0.530–0.643	4	0.155
	e) Susceptibility class 5 (0.041–0.049)	0.644–0.792	5	0.238
	f) Susceptibility class 6 (0.050–0.063)	0.793–1.000	6	0.42
10. Vegetation proportion	a) Susceptibility class 1 (0.471–1.000)	0.00–0.525	1	0.039
	b) Susceptibility class 2 (0.317–0.470)	0.526–0.682	2	0.050
	c) Susceptibility class 3 (0.227–0.316)	0.683–0.772	3	0.068
	d) Susceptibility class 4 (0.156–0.226)	0.773–0.843	4	0.098
	e) Susceptibility class 5 (0.094–0.155)	0.844–0.905	5	0.149
	f) Susceptibility class 6 (0.035–0.093)	0.906–0.964	6	0.222
	g) Susceptibility class 7 (0.000–0.031)	0.965–1.000	7	0.374
11. Land use/land cover	a) Susceptibility class 1 (water bodies)	0.000	1	0.000
	b) Susceptibility class 2 (built-up/dense vegetation)	0.200	2	0.074
	c) Susceptibility class 3 (agricultural land/sparse Vegetation)	0.400	3	0.109
	d) Susceptibility class 4 (fallowland/bushes and scrublands)	0.600	4	0.168
	e) Susceptibility class 5 (bare soil and wasteland)	0.800	5	0.222
	f) Susceptibility class 6 (rock outcroplands)	1.000	6	0.426

Fig. 10 Graphical analysis of the calculated effective weights versus theoretical weight for each landslide susceptibility criterion
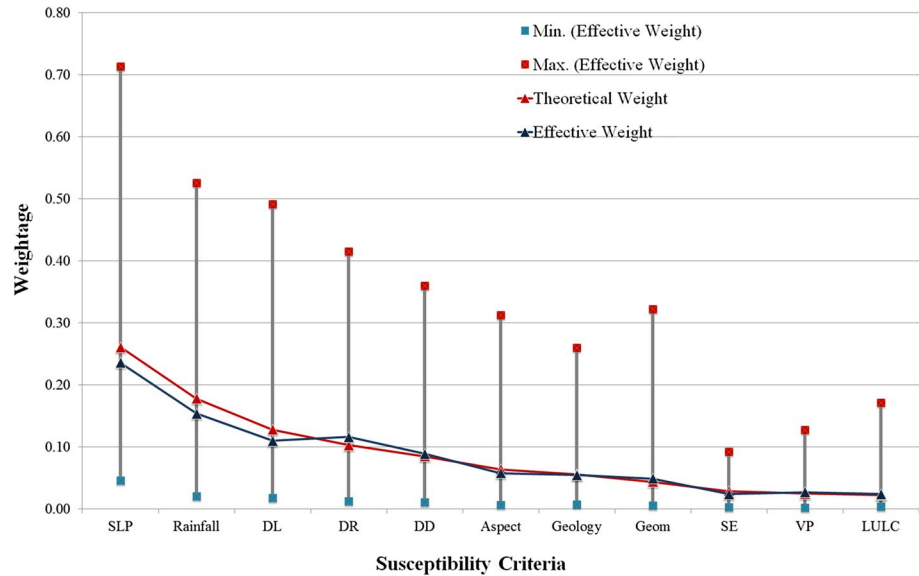
Fig. 11 ROC curve for the proposed landslide susceptibility mapping
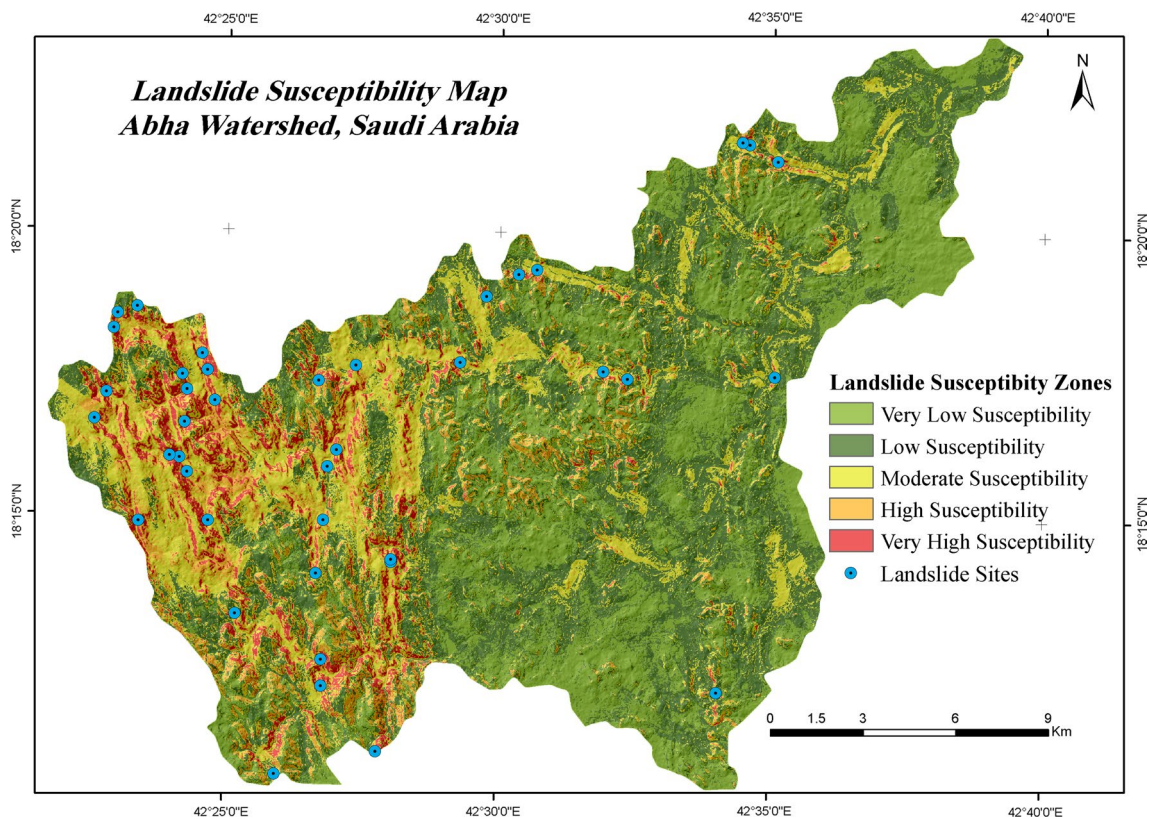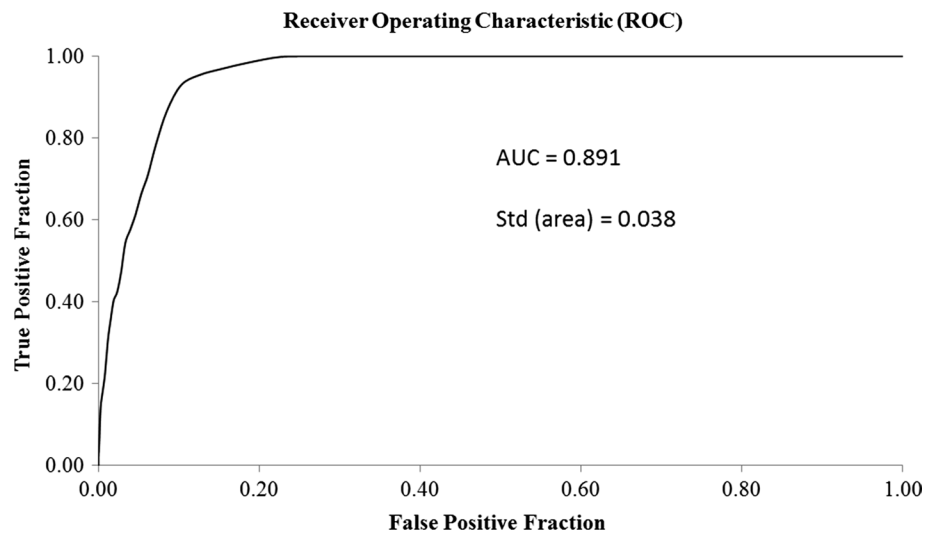
Fig. 12 Landslide susceptibility zones of the watershed

susceptibility area of the watershed has accounted 15.11% area coverage, identifying the steep slope failure susceptible. Concerning quantitative analysis and spatial distribution, the spatial variation of very high and high landslide zones found in the western, south-western and central-north highlands of the watershed. The present study contributes significantly to understanding the watershed hazard susceptibility that could

be used as the preliminary basis by decision makers, planners, and engineers to avoid and minimize the damage and losses caused by existing and future landslides.

The study aimed to integrate the fuzzy set theory with GIS-based AHP-MCDA, which could be a useful tool for incorporating various features that influence the LSM process. The LSM framework emphasizes on structuring the

Table 5 Landslide susceptibility zones of the watershed and their area and percentage of coverage

Class	Landslide susceptibility zone	LSI (range)	Area coverage (km^2)	Area coverage (%)
1	Very low susceptibility	6.24–13.58	99.00	26.76
2	Low susceptibility	13.59–17.18	131.64	35.58
3	Moderate susceptibility	17.19–21.56	83.42	22.55
4	High susceptibility	21.57–27.35	35.27	9.53
5	Very high susceptibility	27.36–39.07	20.67	5.59

decision-making process. The integration of fuzzy-AHP approach used to decide the criteria weightings from the subjective method. The proposed method ascertains that the fuzzy set theory coupled with GIS-based AHP-MCDA can produce a high-reliability landslide hazard map. The fuzzy-AHP approach is promising for GIS-based MCDA as it solves two significant limitations of the conventional AHP. Initially, AHP used in a single process which depends on expert knowledge for assigning the criteria weights while allowing a specific level of subjectivity in the pairwise comparison matrix. Secondly, the inconsistency of the technique has been recognized to a constrained scale of judgment, the absence of transitivity, and the rank reversal phenomenon.

So, it neccessiates to discuss about the AHP and its limitation in the present context. Since in the beginning AHP has been performed in various applications in environmental hazard, hydrogeology, environmental planning and management (Saaty 1980; Chen et al. 2001; Madrucci et al. 2008; Jha et al. 2010; Abba et al. 2013; Mallick et al. 2014). AHP has gained significance in terms of interactive graphical UIs, automatic calculation of priorities and inconsistencies and several ways to process a sensitivity analysis, yet there is still lot of controversy surrounding AHP (Jha et al. 2010; Ahmad et al. 2013). The rank reversal phenomenon arises from inclusion of new alternative or deletion of an old alternative in decision-making process. This results in change of ranking in the past choices. It had been one of the significant constraints of utility-based theories that initially assumed the most imperative component/s of decision-making is/are alternative/s and their utilities under the different criteria (Saaty and Vargas 2008). These issues continued persist until Millet and Saaty (2000) proposed examples where ranking should be preserved or permitted to reverse. The provided examples explained that AHP accommodates two types of blend procedures: ideal mode (allows for alternative rank preservation) and distributive mode (which does allow for rank reversal). The pairwise comparison in AHP utilizes a reliable method of transforming pairwise comparisons into a set of numbers representing the relative priority of each criterion.

Though numerous other scales discussed in the literature, none of them completely address the previously mentioned issues with AHP. A ratio scale proposed by Saaty (1977) was utilized in the utmost applications (Duru et al. 2012). The data uncertainty and the ambiguity of human decision make it difficult to provide correct numerical weights to evaluate the criteria. In many cases, the pairwise comparison ratings can't be chosen precisely and experts may prefer intermediate ratings instead of definite ratings. In order to solve the issue of precision, fuzzy-AHP compares with more adaptable for obtaining experts' preferences (Kahraman et al. 2003; Kutlu and Ekmekçioglu. 2012). In the fuzzy-AHP method, each decision has a specific arrangement, which is related with a two-dimensional priority matrix (viz. criterion vs. criterion). Whereas, conventional AHP utilizes pairwise comparisons of criteria in a top-down sequence and weights choice matrices by the consequence of a single identical priority matrix (Duru et al. 2012). Since the assessment criteria of the best arrangement have the different implications and meanings, there is no legitimate reason to treat them all as of equal importance. Moreover, fuzzy-AHP utilized to deal with the categorical criteria (qualitative data) of LSM (e.g. slope, aspect, geomorphological, geology and LULC) which are difficult to describe in crisp values, thus strengthen the comprehensiveness and reasonableness of the decision-making process (Chen et al. 2011). Fuzzy-AHP calculates both priorities and data by fuzzy sets (Duru et al. 2012).

In the present research, GIS-based fuzzy-AHP-MCDA framework performed to LSM. This research investigates that the framework utilizes artificial values derived through pairwise comparisons. However, Duru et al. (2012) described, various fuzzy-AHP studies which lack of the matrix consistency problem, though the choices are inconsistent. The outcomes of this study show that the combination of fuzzy set theory with AHP in both criteria weighting and normalization. According to our results, it can be stated that the integration of fuzzy sets with AHP in both criteria weighting and normalization gives high adaptability in choices and decision-making. The criteria weighting and normalization also considers the uncertainties in the LSM process by using FMFs as well as by methods for triangular fuzzy numbers (TFNs) rather than crisp numbers for comparing the relative significance between LSM criteria. Moreover, fuzzy logic is appealing because in light of the fact that it is simple to understand and implement. Fuzzy logic can be applied on data for any measurement scale, and the weighting is defined by the expert (Chen et al. 2011; Feizizadeh et al. 2013). Nevertheless, the study presents more practical assessment of landslide susceptibility mapping using linguistic variables. The fuzziness nature of data renders inaccurate assessment which can be overcome successfully by employing fuzzy-AHP weights (Oguzitimur 2011; Mijani and Samani 2017).

Conclusions

Landslides are a natural disaster, significantly affected by the failure of materials making up the hill slopes and augmented by the force of gravity, precipitation and anthropogenic activities. In last few decades, landslides have been considered to be the most critical natural hazards in Aseer region, Saudi Arabia. Therefore, a short- and long-term solution is required for mitigating the landslide risk. The study presents an integrated approach for landslide susceptibility map with prominence on structuring the decision-making process. This could be assessed by appropriate data selection, weighting of criteria and normalization. The integrated GIS-based fuzzy-AHP-MCDA framework applied to landslide prone areas, in order to understand the processes that contribute to the landslides. The proposed method ascertains that the fuzzy set theory coupled with GIS-based AHP-MCDA can produce a high-reliability landslide hazard map. According to study results, it can be stated that the integration of fuzzy sets with AHP in both criteria weighting and normalization gives high adaptability in choices and decision-making. The criteria weighting and normalization also consider the uncertainties in the LSM process by using FMFs as well as by methods for triangular fuzzy numbers (TFNs) rather than crisp numbers for comparing the relative significance between LSM criteria. Moreover, fuzzy logic is appealing because in light of the fact that it is simple to understand and implement.

The study results summarize the weighted overlay analysis method using MCDM. The landslide susceptibility zones identified and mapped into five classes: very low susceptibility, low susceptibility, moderate susceptibility, high susceptibility and very high susceptibility. The analysis shows that very high and high susceptibility area of the watershed has accounted 15.11% area coverage, identifying the steep slope failure susceptible. Concerning spatial distribution, the spatial variation of very high and high landslide zones found in the western, south-western and central-north highlands of the watershed.

The study results and findings illustrated that the stated approach can produce a high-reliability landslide hazard map. However, different uncertainty aspects of LSM need to be resolved. A degree of uncertainty will always persist in any LSM due to the uncertainty inherent in LSM criteria. The uncertainty inherent exists both in the criteria weighting and in degree of influence by each criterion. In order to overcome spatial uncertainty in fuzzy-AHP approach, the future research will evaluate the spatially explicit reliability models for spatial sensitivity and uncertainty analyses based on GIS-fuzzy-AHP MCDA and also the impact of rainfall time series with different length in a landslide susceptibity in the framework of changing rainfall spatio-temporal change. The present study contributes significantly to understanding the watershed hazard susceptibility that could be used as the preliminary basis by decision makers, planners, and engineers to avoid and minimize the damage and losses caused by existing and future landslides. These results will also be useful in explaining the relationship between known landslides and landslide susceptibility, and thereby, it assists geoscientists and engineers in the analysis and design process, sustainable land stability management aimed at mitigation of landslide impacts. The methodology applied herein may be used in landslide susceptibility assessment throughout similar semi-arid watershed environments.

References

Abba AH, Noor ZZ, Yusuf RO, Din MF, Hassan MAA (2013) Assessing environmental impacts of municipal solid waste of Johor by analytical hierarchy process. Resour Conserv Recycl 73:188–196

Abdulaziz MB, Faisal KZ, Mohammad TH (2014) Natural hazards in Saudi Arabia. In: Ismail-Zadeh A, Fucugauchi JU, Kijko A, Takeuchi K, Zaliapin I (eds) Extreme natural hazards, disaster risks and societal implications. Cambridge University Press, Cambridge

Abulfatih HA (1981) Wild plants of Abha and its surroundings. Saudi Publishing and Distributing House, vol 5, pp 125–159

Ahmad HA, Zainura ZN, Rafiu O, Mohd FMD, Mohd AAH (2013) Assessing environmental impacts of municipal solid waste of Johor by analytical hierarchy process. Resour Conserv Recycl 73:188–196

Akgun A, Türk N (2010) Landslide susceptibility mapping for Ayvalik (Western Turkey) and its vicinity by multicriteria decision analysis. Environ Earth Sci 61:595–611

Altrock CV, Krause B (1994) Multi-criteria decision-making in German automotive industry using fuzzy logic. Fuzzy Sets Syst 63(3):375–380

Andreo B, Vías J, Durán JJ, Jiménez P, López-Geta JA, Carrasco F (2008) Methodology for ground water recharge assessment in carbonate aquifers: application to pilot sites in southern Spain. Hydrogeology 16(5):911–925

Arlegui LE, Soriano MA (1998) Characterizing lineaments from satellite images and field studies in the central Ebro basin (NE Spain). Int J Remote Sens 19:3169–3185

Ayalew L, Yamagishi H, Ugawa N (2004) Landslide susceptibility mapping using GIS-based weighted linear combination, the case in Tsugawa area of Agano River, Niigata Prefecture, Japan. Landslides 1:73–81

Balezentiene L, Streimikiene D, Balezentis T (2013) Fuzzy decision support methodology for sustainable energy crop selection. Renew Sustain Energy Rev 17:83–93

Barredo J, Benavides A, Hervas J, VanWesten CJ (2000) Comparing heuristic landslide hazard assessment techniques using GIS in the Tirajana basin, Gran Canaria Island, Spain. Int J Appl Earth Obs Geoinf 2:9–23

Berhanu B, Melesse AM, Sleshi Y (2013) GIS-based hydrological zones and soil geo-database of Ethiopia. Catena. https://doi.org/10.1016/j.catena.2012.12.007

Brabb E (1984) Innovative approaches for landslide hazard evaluation. In: IV international symposium on landslides, Toronto, pp 307–323

Buckley JJ (1985) Fuzzy hierarchical analysis. Fuzzy Sets Syst 17(1):233–247

Cammeraat LH, Imeson AC (1999) The evolution and significance of soil-vegetation patterns following land abandonment and fire in Spain. Catena 37:107–127

Cardinali M, Reichenbach P, Guzzetti F, Ardizzone F, Antonini G, Galli M, Cacciano M, Castellani M, Salvati P (2002) A geomorphological approach to estimation of landslide hazards and risks in Umbria, Central Italy. Nat Hazards Earth Syst Sci 2:57–72. https://doi.org/10.5194/nhess-2-57-2002

Carlos AB, Odette IJ (2012) Soil erodibility mapping and its correlation with soil properties in central Chile. Geoderma 189–190:116–123

Carrara A (1983) Multivariate models for landslide hazard evaluation. J Int Assoc Math Geol 15:403–426

Carter MR (1993) Soil sampling and methods of analysis. Canadian society of soil science, Lewis Publishers, Charlottetown

Carver SJ (1991) Integrating multi-criteria evaluation with geographical information systems. Int J Geogr Inf Syst 5(3):321–339

Chen K, Blong R, Jacobson C (2001) MCE-RISK: integrating multicriteria evaluation and GIS for risk decision-making in natural hazards. Environ Model Softw 16:387–397

Chen Y, Yu J, Khan S (2010) Spatial sensitivity analysis of multi-criteria weights in GIS-based land suitability evaluation. Environ Modell Softw 25(12):1582–1591

Chen VYC, Pang Lien H, Liu CH, Liou JJH, Hshiung Tzeng G, Yang LS (2011) Fuzzy MCDM approach for selecting the best environment-watershed plan. Appl Soft Comput 11:265–275

Cheung FKT, Kuen JLF, Skitmore M (2002) Multi-criteria evaluation model for the selection of architecture consultants. Constr Manag Econ 20(7):569–580

Chowdhury A, Jha MK, Chowdary VM, Mal BC (2009) Integrated remote sensing and GIS-based approach for assessing ground water potential in West Medinipur District, West Bengal, India. Int J Remote Sens 30(1):231–250

Constantin M, Bednarik M, Jurchescu MC, Vlaicu M (2011) Landslide susceptibility assessment using the bivariate statistical analysis and the index of entropy in the Sibiciu Basin (Romania). Environ Earth Sci 2011(63):397–406. https://doi.org/10.1007/s12665-010-0724-y

Dou J, Yamagishi H, Pourghasemi HR, Yunus AP, Song X, Xu Y, Zhu Z (2015) An integrated artificial neural network model for the landslide susceptibility assessment of Osado Island, Japan. Nat Hazards 78:1749–1776

Duman TY, Can T, Gokceoglu C, Nefeslioglu HA (2005) Landslide susceptibility mapping of Cekmece area (Istanbul, Turkey) by conditional probability. Hydrol Earth Syst Sci Discuss 2:155–208

Duru O, Bulut E, Yoshida S (2012) Regime switching fuzzy AHP model for choicevarying priorities problem and expert consistency prioritization: a cubic fuzzypriority matrix design. Expert Syst Appl 39:4954–4964

Dwivedi RS, Sreenivas K, Ramana KV (2005) Land-use/land-cover change analysis in part of Ethiopia using Landsat Thematic Mapper data. Int J Remote Sens 26(7):1285–1287

Feizizadeh B, Blaschke T (2013) GIS-multicriteria decision analysis for landslide susceptibility mapping: comparing three methods for the Urmia lake basin, Iran. Nat Hazards 65:2105–2128

Feizizadeh B, Blaschke T, Nazmfar H, Rezaei Moghaddam MH (2013) Landslide susceptibility mapping for the Urmia Lake basin, Iran: a multi-criteria evaluation approach using GIS. Int J Environ Res 7(2):319–3336

Feizizadeh B, Roodposhti MS, Jankowski P, Blaschke T (2014) A GIS-based extended fuzzy multi-criteria evaluation for landslide susceptibility mapping. Comput Geosci 73:208–221

Gomez B, Jones PJ (2010) Research methods in geography—a critical introduction. Wiley, Chichester

Gorsevski PV, Jankowski P (2010) An optimized solution of multicriteria evaluation analysis of landslide susceptibility using fuzzy sets and Kalman filter. Comput Geosci 36:1005–1020

Greenwood WR (1985) Geologic map of the Abha quadrangle, sheet 18 F. Kingdom of Saudi Arabia, Ministry of Petroleum and Mineral Resources, Deputy Ministry for Mineral Resources GM-75 c, scale 1:250,000

GSI and NRSC (2010) Manual for national geomorphological and lineament mapping on 1:50,000 scale (Document control number: NRSC-RS&GISAA-ERG-G&GD-FEB' 10- TR149). National Remote Sensing Centre, Hyderabad

Guzzetti F, Mondini AC, Cardinali M, Fiorucci F, Santangelo M, Chang KT (2012) Landslide inventory maps: new tools for an old problem. Earth Sci Rev 112(1–2):42–66

Guzzetti F, Reichenbach P, Ardizzone F, Cardinali M, Galli M (2006) Estimating the quality of landslide susceptibility models. Geomorphology 81:166–184

Hill J, Schutt B (2000) Mapping complex patterns of erosion and stability in dry Mediterranean ecosystems. Remote Sens Environ 74:557–569

Hong H, Pradhan B, Xu C, Bui DT (2015) Spatial prediction of landslide hazard at the Yihuang area (China) using two-class kernel logistic regression, alternating decision tree and support vector machines. Catena 133:266–281

Hsieh TY, Lu ST, Tzeng GH (2004) Fuzzy MCDM approach for planning and design tenders selection in public office buildings. Int J Project Manage 22(7):573–584

Ilanloo M (2011) A comparative study of fuzzy logic approach for landslide susceptibility mapping using GIS: an experience of Karaj dam basin in Iran. In: The 2nd international geography symposium-mediterranean environment. Proc Soc Behav Sci 19, 668–676

Intarawichian N, Dasananda S (2010) Analytical Hierarchy Process for landslide susceptibility mapping in lower Mae Chem watershed, Northern Thailand. Suranaree J Sci Technol 17(3):277–292

Ishizaka A, Labib A (2011) Review of the main developments in the analytic hierarchy process. Expert Syst Appl 38:14336–14345

Jensen JR (2005) Introductory digital image processing: a remote sensing perspective, 3rd edn. Prentice-Hall, Upper Saddle River

Jha MK, Chowdary VM, Chowdhury A (2010) Groundwater assessment in Salboni Block, West Bengal (India) using remote sensing, geographical information system and multi-criteria decision analysis techniques. Hydrogeol J 18(7):1713–1728

Kahraman C, Cebeci U, Ulukan Z (2003) Multi-criteria supplier selection using fuzzy AHP. Logist Inf Manage 16(6):382–394

Katz O, Morgan JK, Aharonov E, Dugan B (2014) Controls on the size and geometry of landslides: insights from discrete element numerical simulations. Geomorphology 220:104–113

Kutlu AC, Ekmekçioglu M (2012) Fuzzy failure modes and effects analysis by using fuzzy TOPSIS-based fuzzy AHP. J Expert Syst Appl 39:61–67

Lee S (2004) Application of likelihood ratio and logistic regression models to landslide susceptibility mapping using GIS. Environ Manage 34(2):223–232

Lee S, Min K (2001) Statistical analysis of landslide susceptibility at Yongin, Korea. Environ Geol 40:1095–1113. https://doi.org/10.1007/s002540100310

Lee S, Choi J, Woo I (2004a) The effect of spatial resolution on the accuracy of landslide susceptibility mapping: a case study in Boun, Korea. Geosci J 8:51–60

Lee S, Ryu JH, Won JS, Park HJ (2004b) Determination and application of the weights for landslide susceptibility mapping using an artificial neural network. Eng Geol 71:289–302

Li SP, Will BF (2005) A fuzzy logic system for visual evaluation. Environ Plan 32(2):293–304

Lillesand TM, Kiefer RW (1999) Remote sensing and image interpretation. Wiley, New York

Liu B (2004) Uncertainty theory: an introduction to its axiomatic foundations. Springer, Berlin

Lu GY, Wong DW (2008) An adoptive inverse-distance weighting spatial interpolation techniques. Comput Geosci 34:1044–1055

Madrucci V, Taioli F, De Araújo CC (2008) Groundwater favourability map using GIS multicriteria data analysis on crystalline terrain, São Paulo State, Brazil. J Hydrol 357:153–173

Maerz NH, Youssef AM, Pradhan B, Bulkhi A (2014) Remediation and mitigation strategies for rock fall hazards along the highways of Fayfa Mountain, Jazan Region, Kingdom of Saudi. Arab J Geosci. https://doi.org/10.1007/s12517-014-1423-x

Malczewski J (1999) GIS and multicriteria decision analysis. Wiley, New York, p 392

Malczewski J (2004) On the use of weighted linear combination method in GIS: common and best practice approaches. Trans GIS 4(1):5–22

Mallick J (2016) Geospatial-based soil variability and hydrological zones of Abha semi-arid mountainous watershed, Saudi Arabia. Arab J Geosci 9:281. https://doi.org/10.1007/s12517-015-2302-9

Mallick J, Alashker Y, Shams M, Mohd A, Mohd AH (2014) Risk assessment of soil erosion in semi-arid mountainous watershed in Saudi Arabia by RUSLE model coupled with remote sensing and GIS. Taylor and Francis, Oxford, pp 1–26

Mandal S, Maiti R (2014) Role of lithological composition and lineaments in landsliding: a case study of Shivkhola watershed, Darjeeling Himalaya. Int J Geol Earth Environ Sci 4(1):126–132

Marinoni O, Higgins A, Hajkowicz S, Collins K (2009) The multiple criteria analysis tool (MCAT): a new software tool to support environmental investment decision making. Environ Modell Softw 24(2):153–164

Mason PJ, Rosenbaum M (2002) Geohazard mapping for predicting landslides: an example from the Langhe Hills in Piemonte, NW Italy. Q J Eng Geol Hydrogeol 35:317–326

Mcintyre C, Parfitt MK (1998) Decision support system for residential land development site selection process. J Archit Eng 4(4):125–131

Mijani N, Samani NN (2017) Comparison of fuzzy-based models in landslide hazard mapping. The international archives of the photogrammetry, remote sensing and spatial information sciences, XLII-4/W4, pp 407–416

Millet I, Saaty TL (2000) On the relativity of relative measures—accommodating both rank preservation and rank reversal in the AHP. Eur J Oper Res 121:205–212

Nalbant S, Alptekin O (1995) The use of Landsat Mapper imagery for analyzing lithology and structure of Korucu-Dugla area in western Turkey. Int J Remote Sens 16(13):2357–2374

Nandi A, Shakoor A (2010) A GIS-based landslide susceptibility evaluation using bivariate and multivariate statistical analyses. Eng Geol 110(1):11–20

Napolitano P, Fabbri AG (1996) Single-parameter sensitivity analysis for aquifer vulnerability assessment using DRASTIC and SINTACS. In: Proceedings of the Vienna conference on HydroGIS 96: application of geographic information systems in hydrology and water resources management, IAHS Pub. No. 235, pp 559–566

Neaupane KM, Piantanakulchai M (2006) Analytic network process model for landslide hazard zonation. Eng Geol 85:281–294

Nicholas MS (2005) The remote sensing tutorial, NASA's Goddard, USA. http://www.ucl.ac.uk/EarthSci/people/lidunka/GEOL2014/Geophysics%2010%20-Remote%20sensing/Remote%20Sensing%20Tutorial%20Overview.htm. Accessed 31 Mar 2018

Oguzitimur S (2011) Why fuzzy analytic hierarchy process approach for transport problems? In: European regional science association ERSA conference papers, Aug 2–6, 1090 Vienna, Austria, ersa11, p 438

Ohta K, Kobashi G, Takato S, Kagaya S, Yamada H, Minakami H, Yamamura E (2007) Analysis of the geographical accessibility of neurosurgical emergency hospitals in Sapporo city using GIS and AHP. Int J Geogr Inf Sci 21(6):687–698

Oikonomidis D, Dimogianni S, Kazakis N, Voudouris K (2015) A GIS/remote sensing-based methodology for groundwater potentiality assessment in Tirnavos area, Greece. J Hydrol 525:197–208

Opricovic S, Tzeng GH (2003) Defuzzification within a fuzzy multicriteria decision model. Int J Uncertain Fuzziness Knowl Syst 11:635–652

Ouma Y, Tateishi R (2014) Urban flood vulnerability and risk mapping using integrated multi-parametric AHP and GIS: methodological overview and case study assessment. Water 6(6):1515–1545

Pourghasemi HR, Mohammady M, Pradhan B (2012) Landslide susceptibility mapping using index of entropy and conditional probability models in GIS: safarood Basin, Iran. Catena 97:71–84

Pourghasemi HR, Moradi HR, Fatemi Aghda SM (2013) Landslide susceptibility mapping by binary logistic regression, analytical hierarchy process, and statistical index models and assessment of their performances. Nat Hazards 69:749–779. https://doi.org/10.1007/s11069-013-0728-5

Pradeep KS, Kumar S, Singh RP (2000) Neotectonic study of Ganga and Yamunatear faults, NW Himalaya using remote sensing and GIS. Int J Remote Sens 21:499–518

Pradhan B (2013) A comparative study on the predictive ability of the decision tree, support vector machine and neuro-fuzzy models in landslide susceptibility mapping using GIS. Comput Geosci 51:350–365

Pradhan B, Lee S (2010) Regional landslide susceptibility analysis using back-propagation neural network model at Cameron Highland, Malaysia. Landslides 7:13–30

Rahaman SA, Abdulajeez S, Aruchamy S, Jegankumar R (2015) Prioritization of Sub watershed based on morphometric characteristics using fuzzy analytical hierarchy process and geographical information system—a study of Kallar watershed, Tamil Nadu. Aquat Proc 4:1322–1330

Renard KG, Foster GR, Weesies GA, McCool DK, Yoder DC (1997) Predicting soil erosion by water: a guide to conservation planning with the revised universal soil loss equation (RUSLE). US Department of Agriculture (editor). Washington (DC): US Department of Agriculture. Agricultural Handbook, vol 703, pp 1–251

Roodposhti MS, Rahimi S, Beglou MJ (2014) PROMETHEE II and fuzzy AHP: an enhanced GIS-based landslide susceptibility mapping. Nat Hazards 73:77–95

Roodposhti MS, Aryal J, Shahabi H, Safarrad T (2016) Fuzzy shannon entropy: a hybrid GIS-based landslide susceptibility mapping method. Entropy 18:343. https://doi.org/10.3390/e18100343

Saaty TL (1977) A scaling method for priorities in hierarchical structure. J Math Psychol 15(3):34–39

Saaty TL (1980) The analytic hierarchy process. McGraw-Hill, New York

Saaty TL, Vargas LG (2008) Prediction, projection and forecasting, vol 251. Kluwer, Dordrecht

Shahabi H, Hashim M (2015) Landslide susceptibility mapping using GIS-based statistical models and Remote sensing data in tropical environment. Sci Rep 5:9899

Sheldrick BH, Wang C (1993) Particle size distribution. In: Carter MR (ed) Soil sampling and methods of analysis. Canadian society of soil science, Lewis, Ann Arbor (MI), pp 499–511

Singh BR, Singh S, Singh P, Mishra DK (2014) A study on geomorphological response for runoff prediction in small watershed. IOSR J Comput Eng (IOSR-JCE) e-ISSN: 2278– 0661, p-ISSN: 2278–8727, volume 16, issue 4, version VI (Jul–Aug 2014), pp 86–94

Suzan ML, Toprak V (1998) Filtering of satellite images in geological lineament analyses: an application to a fault zone in central Turkey. Int J Remote Sens 19:1101–1114

Swets JA (1988) Measuring the accuracy of diagnostic systems. Science 240:1285–1293

Tarboton DG, Bras RL, Rodriguez I (1991) On the extraction of channel networks from digital elevation data. Hydrol Process 5:81–100

Valor E, Caselles V (1996) Mapping land surface emissivity from NDVI. Application to European, African and South American areas. Remote Sens Environ 57:167–184

Van Westen CJ, Van Asch TWJ, Soeters R (2006) Landslide hazard and risk zonation—why is it still so difficult? Bull Eng Geol Environ 65:167–184. https://doi.org/10.1007/s10064-005-0023-0

Vincent P (2008) Saudi Arabia: an environmental overview. Taylor and Francis, London. https://doi.org/10.1201/9780203030882

Wang WD, Guo J, Fang LG, Chang XS (2012) A subjective and objective integrated weighting method for landslides susceptibility mapping based on GIS. Environ Earth Sci 65:1705–1714

Wheater HS, Larentis P, Hamilton GS (1989) Design rainfall characteristics for south-west of Saudi Arabia. In: Proceedings of the Institution of Civil Engineers, Part 2, pp 517–538

Willey HB (1979) Fuzzy theory and environmental control in buildings. Environ Plan B 6(3):279–291

Williams CJ, Lee SS, Fisher RA, Dickerman LH (1999) A comparison of statistical methods for prenatal screening for Down syndrome. Appl Stoch Models Data Anal 15:89–101

Wischmeier WH, Smith DD (1978) Predicting rainfall erosion losses—a guide to conservation planning agriculture handbook no 537. US Department of Agriculture Science and Education Administration, Washington, DC

Xu C (2015) Preparation of earthquake-triggered landslide inventory maps using remote sensing and GIS technologies: principles and case studies. Geosci Front 6:825–836

Yalcin A (2008) GIS-based landslide susceptibility mapping using analytical hierarchy process and bivariate statistics in Ardesen (Turkey): comparisons of results and confirmations. Catena 72:1–12

Yalcin A, Bulut F (2007) Landslide susceptibility mapping using GIS and digital photogrammetric techniques: a case study from Ardesen (NE-Turkey). Nat Hazards 41:201–226. https://doi.org/10.1007/s11069-006-9030-0

Yalcin A, Reis S, Aydinoglu AC, Yomralioglu T (2011) A GIS-based comparative study of frequency ratio, 875 analytical hierarchy process, bivariate statistics and logistics regression methods for landslide susceptibility mapping in Trabzon, NE Turkey. Catena 85:274–287. https://doi.org/10.1016/j.catena.2011.01.014

Yilmaz I (2009) A case study from Koyulhisar (Sivas-Turkey) for landslide susceptibility mapping by artificial neural networks. Bull Eng Geol Environ 68(3):297–306. https://doi.org/10.1007/s10064-009-0185-2

Youssef AM, Maerz N (2013) Overview of some geological hazards in the Saudi Arabia. Environ Earth Sci 70:3115–3130. https://doi.org/10.1007/s12665-013-2373-4

Youssef AM, Maerz HN, Al-Otaibi AA (2012) Stability of rock slopes along Raidah Escarpment Road, Aseer Area, Kingdom of Saudi Arabia. J Geogr. https://doi.org/10.5539/jgg.v4n2p48

Youssef AM, Al-kathery M, Pradhan B (2014) Landslide susceptibility mapping at Al-Hasher Area, Jizan (Saudi Arabia) using GIS-based frequency ratio and index of entropy models. Geosci J. https://doi.org/10.1007/s12303-014-0032-8

Youssef AM, Al-kathery M, Pradhan B (2015a) Assessment of impact of mass movements on the upper Tayyah valley's bridge along Shear escarpment highway, Asir region (Saudi Arabia) using remote sensing data and field investigation. Nat Hazards Earth Syst Sci Discuss 3:497–533

Youssef AM, Pourghasemi HR, Pourtaghi ZS, Mohamed M (2015b) Landslide susceptibility mapping using random forest, boosted regression tree, classification and regression tree, and general linear models and comparison of their performance at Wadi Tayyah Basin, Aseer Region, Saudi Arabia. Landslides 13:839–856. https://doi.org/10.1007/s10346-015-0614-1

Youssef AM, Pourghasemi HR, El-Haddad BA, Dhahry BK (2016) Landslide susceptibility maps using different probabilistic and bivariate statistical models and comparison of their performance at Wadi Itwad Basin, Aseer Region, Saudi Arabia. Bull Eng Geol Environ 75:63–87

Zadeh LA (1965) Fuzzy sets. Inf Control 8:338–353